Abdu *Progress in Earth and Planetary Science* (2019) 6:11
https://doi.org/10.1186/s40645-019-0258-1

Progress in Earth and Planetary Science

REVIEW Open Access

Day-to-day and short-term variabilities in the equatorial plasma bubble/spread F irregularity seeding and development

Mangalathayil Ali Abdu[1,2]

Abstract

The background ionospheric conditions shaped by sunset electrodynamic processes are responsible for the development of equatorial plasma bubble (EPB)/equatorial spread F (ESF) irregularities of the post-sunset ionosphere. Distinct conditions exist for the EPB/ESF development also at later hours of the night. The plasma instability growth leading to EPB generation is dependent on the basic precursor conditions defined by the well-known parameters: the evening prereversal enhancement in vertical plasma drift (PRE), wave structure in plasma density and polarization electric field required to initiate/seed the instability, and the F layer bottom side density gradient, as a significant factor in controlling the growth rate. Competing roles of the zonal versus meridional thermospheric winds additionally control their development. Statistical as well as case studies have addressed aspects of the EPB development and occurrence under different geophysical conditions, generally focusing attention on any one of the above specific parameters. Little is known regarding the relative importance of concurrent presence of the precursor parameters (mentioned above) in shaping a given event. A large degree of day-to-day variability in these parameters arise from different sources of forcing, such as upward propagating atmospheric waves, and magnetic disturbance time electric fields in the form of prompt penetration and disturbance dynamo electric fields that often contribute to the widely observed short-term variabilities in EPB development and dynamics. In this paper, we will present and discuss some important aspects of the EPB/ESF short-term variability, focusing attention on their enhanced development, or suppression and, wherever possible, highlighting also the relative roles of the precursor parameters in such variability.

Keywords: Equatorial ionosphere, Plasma bubbles/spread F irregularities, Prereversal vertical drift, Prompt penetration electric field, Gravity waves, Trans-equatorial wind, Planetary/Kelvin waves, ESF/EPB short-term variability

Introduction

The nighttime equatorial ionospheric plasma structuring manifests itself in the form of geomagnetic field-aligned plasma irregularities, also known by its generic name as equatorial spread F (ESF) or equatorial plasma bubble (EPB) irregularities. The ESF/EPB irregularities occur in a wide spectrum of scale sizes (from few centimeters to a few hundreds of kilometers); the shortest scale measured being 11 cm (Tsunoda 1980) and the outer scale size reaching 800–1000 km. They also present a large degree of variability with wide-ranging time scales. The long-term variability in their development and occurrence is dependent largely on solar activity cycle defined by the variations in solar EUV flux and/or sunspot number. The medium-term variability is dependent on the season as well as solar flux, and it is by far relatively better understood and therefore more easily predictable. There are also short-term variabilities in the form of changes occurring on a day-to-day basis, as well as of a more transient nature in response to their driving sources with corresponding time scales. Upward propagating atmospheric waves, such as, gravity waves, and planetary waves, produce variabilities on time scales varying from short-term to several days of quasi periods. It is reasonable to consider that the shorter term and day-to-day variabilities could be largely controlled by gravity waves, whereas

Correspondence: abdu.managa@gmail.com
[1]Instituto Tecnológico de Aeronáutica (ITA), São Jose dos Campos, Brazil
[2]Instituto Nacional de Pesquisas Espaciais (INPE), São Jose dos Campos, Brazil

the variability on time scale of a few to several days could be largely driven by planetary/Kelvin waves through their modulation of tidal winds. The variabilities arising from magnetospheric (and high latitude) forcing can also be of transient nature with time scales varying from minutes to hours, or of several days. Little is known about the different drivers of these short-term and day-to-day variabilities, which therefore are the least predictable component of the ESF variability. Investigations on the sources and characteristics of the variabilities are important due, primarily, to the impacts of these irregularities and the background ionospheric conditions on the different space application systems of practical interest to us. Further, a better understanding of the possible drivers of such variabilities is a primary requirement for advancing our knowledge on the science of the coupling processes that govern their development as well as to make continuing progress towards developing predictive capability on their occurrences.

The irregularities originate from plasma instability process that may develop in the nighttime ionosphere when conditions of the background ionosphere are favorable for their development. In the most typical scenario, the instability may develop through the Rayleigh-Taylor interchange mechanism (Dungey 1956) acting on the seed perturbations in density and polarization electric field produced by gravity waves at the bottom side of a rapidly rising post-sunset F layer. The rapid post-sunset rise of layer (PSSR) occurs through the enhanced vertical plasma drift arising from the evening prereversal enhancement in the zonal electric field (the PRE). The PRE is generated through the action of the F layer dynamo under sunset electrodynamics processes. The thermospheric zonal wind, which is eastward in the evening, produces vertical polarization electric field in the F region that has strong longitudinal gradient across the sunset terminator due to the decay in the E layer conductivity towards the nightside. This situation leads to the development of the PRE as explained by Rishbeth (1971) (see also Heelis et al. 1974; Farley et al. 1986; Eccles et al. 2015). Based on a TIECGM simulation study, a candid explanation of the PRE development was recently presented by Heelis et al. (2012). During low solar flux years, the PRE vertical drift velocity is relatively small, when therefore the role of an instability seed source may become relatively more important for the ESF development. The instability seeding through perturbations in electron density and polarization electric field is believed to be provided by gravity waves propagating upward from sources of their likely generation in the tropospheric convective regions (see for example, Rottger 1981; Huang et al. 1993; Mc Clure et al. 1998; Fritts and Vadas 2008; Abdu et al. 2009a; Tsunoda 2010; Li et al. 2016). Once initiated at the F layer bottom side gradient region under sufficiently large linear growth rate condition, the instability may grow nonlinearly to topside ionosphere in the form of plasma-depleted magnetic field-aligned structures. These structures may cascade into a wide spectrum of scale sizes of irregularities (Haerendel 1973), the composite form of which is known by the generic name, the ESF irregularities, that are observable by a wide variety of diagnostic techniques. Being part of the coupled atmosphere-ionosphere-thermosphere system, they suffer variabilities due to different sources of forcing related to magnetospheric disturbances and lower atmospheric wave activities. As a result, large degrees of day-to-day and short-term variabilities mark the development and occurrence of the EPB/ESF irregularities, which constitute the prime focus of this paper.

Plasma bubble/ESF generation mechanism

The EPB/ESF irregularity development takes place in sequential phases, the observed details of which can vary depending upon the diagnostic techniques. The earliest observation by ionosondes (Booker and Wells 1938) showed that the rise of the post-sunset F layer to higher altitudes was a precondition for the occurrence of range spread F echoes in ionogram. The observations also revealed that the presence of satellite traces adjacent to the main F layer trace in ionogram was often a precursor to the spread F (SF) development (Lyon et al. 1961; Abdu et al. 1981; Tsunoda 2008). The range-time-intensity (RTI) map obtained by the Jicamarca VHF radar showed that the generation of 3-m irregularities was initiated at the F layer bottom side. Their upward growth to the topside ionosphere provided the first indication that the ESF irregularities are associated with magnetic field-aligned plasma depletions, that is, plasma bubbles, that rise upward from the F layer bottomside following their generation through the Rayleigh-Taylor (R-T) interchange instability mechanism (Woodman and La Hoz 1976; Woodman 2009; Scannapieco and Ossakow 1976; Hanson and Sanatani 1971). Diagnostics by the ALTAIR fully steerable incoherent scatter radar (at UHF) has provided important information on the characteristics of the two-dimensional background conditions propecious for the irregularity growth and evolution. A notable precursor condition was identified as the post-sunset upwelling of the F layer having characteristics of a large-scale wave structure (LSWS) (e.g., Tsunoda et al. 1979; Tsunoda and White 1981). From east-west scan measurements in the equatorial plane, it was observed that the irregularities first developed at the west wall of the upwelling, which was attributed to instability growth through zonal wind interaction with the horizontal gradient region of the upwelling or that of associated wave structure. Based on ALTAIR results complemented by results from other

instruments (such as ionosondes and optical imagers), Tsunoda (2015) further characterized the EPB generation process as occurring in three phases: (1) amplification of the upwelling during the post-sunset rise of the *F* layer (due to prereversal vertical drift, PRE), (2) launching of the EPB from the crest of the upwelling, and (3) structuring of the plasma within the upwelling. The ALTAIR observations further revealed that EPBs occurred often in clusters that are connected with the ESF patches in the bottom side F layer and that their zonal widths were comparable to those of the upwelling. Considerations on the day-to-day variability in the background conditions and on the drivers that contribute to the phases defining the EPB/ESF development, especially those related to the phases (1) and (2) above, constitute the key elements of the discussion to follow in this paper. Central to the discussion to begin with is the basic plasma instability mechanism responsible for the generation of the EPB/ESF irregularities, that is, the Rayleigh-Taylor (R-T) interchange mechanism. A comprehensive picture of the EPB generation mechanism and the different sources of forcing that can modify the coupled processes leading to the EPB short-term variability is presented schematically in Fig. 1. The red colored blocks represent the parameters that play direct roles in the processes leading to the EPB generation. Their relationship contributing to the instability linear growth rate (γ_{FT}) through the generalized Rayleigh-Taylor mechanism can be expressed through field line integrated parameters as given by Eq. 1 (Sultan 1996)

$$\gamma_{FT} = (1/L_{FT})\left(\Sigma_P{}^F/\Sigma_P{}^F + \Sigma_P{}^E\right) \times \left(E/B - U^P{}_{FT} + g/\nu_{in}\right) - \beta_{FT} \quad (1)$$

Each of terms in Eq. 1 is represented as a corresponding box in Fig. 1. The term E/B represents the evening prereversal vertical drift marked as PRE in Fig. 1; g is the gravitational acceleration; ν_{in} is the ion-neutral collision frequency, with the gravity term g/ν_{in} also shown in the figure; and L_{FT} is the F layer flux tube integrated bottom side gradient scale length, shown in the figure box also as such, (which has its simplified local form expressed as $N_i/(\Delta N_i/\Delta h)$, where N_i is the ion density). The ratio of F region field line integrated conductivity to the sum of the E and F region-integrated conductivities, $(\Sigma_P{}^F/(\Sigma_P{}^F + \Sigma_P))$, in Eq. 1 is shown as such in the figure box. $\boldsymbol{\beta}_{FT}$ is the recombination rate (not shown in the Figure). U^P_{FT} is the meridional wind in the vertical plane marked as such in the figure box, which can also be part of a trans-equatorial wind (TEW). We may further note that (1) the conductivity ratio (in Eq. 1) increases from a fraction of one before sunset to one as the E layer conductivity decays into the night, (2) the linear growth rate increases with decrease in gradient length, and (3) both the PRE

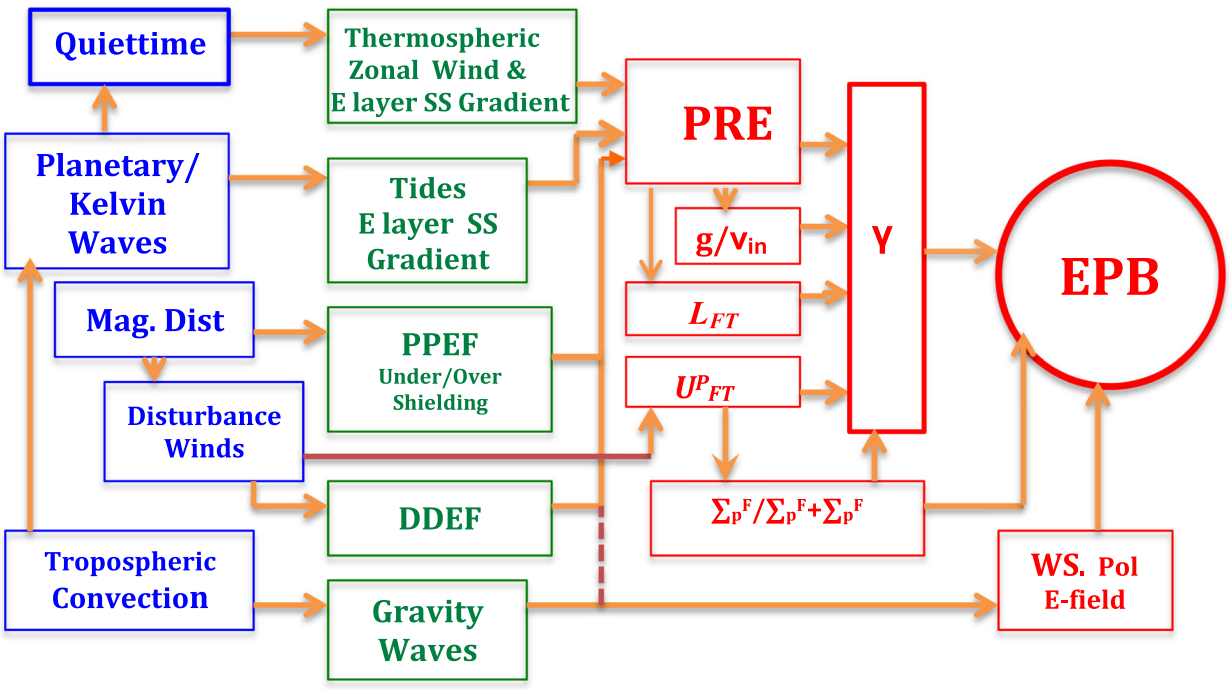

Fig. 1 A schematic representation of the coupled processes controlling the EPB/ESF development and its short-term variabilities. The boxes in red show the connection among the specific background parameters (explained in the text) that determine the EPB growth through R-T instability linear growth rate. The green boxes depict the parameters that modify/control the basic parameters responsible for EPB generation. The blue boxes specify the sources of forcing that operate in the different types of the short-term variabilities as explained in the text

vertical drift and the gravity terms contribute positively to the linear growth rate while the meridional wind term contributes mostly negatively to γ_{FT}. It is to be noted further that the contribution to $\boldsymbol{\gamma_{FT}}$ arising from the PRE vertical drift has additional aspects: (a) an increase in E/B can result in an increase in the gravity term (g/ν_{in}) due to the decrease in the ion-neutral collision frequency as the F layer height rises due to the PRE, the gravity term thereby further raising the γ_{FT}, and (b) the gradient scale length has been found to increase with increase in F layer height, so that an increase in E/B (that raises the F layer height) can contribute to an increase in the gradient scale length (L_{FT}) that, in turn, could contribute to slow down the growth rate. We may point out that the linear growth rate is derived from one-dimensional perturbation analysis in which the seed perturbation is assumed not to perturb the background conditions represented as field line-integrated quantities. Therefore, if the linear growth rate so obtained is found to be above a threshold value, instability growth could occur (in the form of structure amplitude growth) along the entire field line. Considering the equatorial plane two-dimensional situation, such growth should be favored at the crest of the upwelling depending upon the degree to which the LSWS may modulate the larger scale upwelling of evening F layer produced by the PRE (to be further commented later). Even when the linear growth rate is large enough, the instability may develop only if a seed perturbation of sufficient amplitude is present. The seed perturbation can be in the form of a wave structure in density and polarization electric field (indicated in the fig. box as WS. Pol E-field), which may be induced by gravity waves, as depicted in the figure. Another form of seeding process has been suggested as that arising from instability growth in the shear flow region of the post-sunset plasma vortex. As discussed by Kudeki and Bhattacharyya (1999) and Hysell and Kudeki (2004), the westward plasma flow in the presence of eastward neutral wind in the bottomside/valley region of the F layer (below the plasma vortex focus) can be an important energy source for creating an instability that may provide the seed perturbation capable of initiating EPB development by the R-T mechanism. Nonlinear growth of the instability (from a background condition already distorted by the linear growth process) may lead to a more rapid rise of bubble structures to topside ionosphere. However, such nonlinear growth can be retarded/limited by the field line integrated conductivity that is controlled (mostly increased) by meridional/trans-equatorial winds. It should be pointed out that the linear growth rate expression stated above was derived on assumption of small perturbations, with higher order terms discarded (see Sultan 1996, for details) so that it represents only a tendency for the instability growth. As a result, discrepancy may be expected between a specific ESF observation and the linear growth rate that predicted its development.

The parameters indicated in the top green box of Fig. 1, namely, the thermospheric zonal wind and the E layer conductivity sunset (SS) gradient in the evening hours, are the ones directly responsible for the development of the evening prereversal vertical drift enhancement (the PRE). The other green boxes indicate the parameters that may, directly or indirectly, modify the intensity of the PRE and thereby the factors (or terms) that determine the linear and nonlinear growth rates for the EPB. These parameters, which we call as "modifying parameters" are (1) prompt penetration electric fields (PPEF), (2) disturbance dynamo electric field (DDEF), (3) tidal winds modifying the sunset gradient in the E layer conductivity, and (4) gravity waves. They can suffer large degrees of short-term changes as a result of the variabilities in the sources driving them (driving sources), represented in blue boxes in Fig. 1. These drivers are magnetospheric disturbances and upward propagating wave disturbances originating from the lower atmosphere. The latter is dominated by upward propagating atmospheric waves in the form of gravity waves and planetary/Kelvin waves originating from tropospheric convection processes. The planetary waves (PWs) are very large horizontal scale atmospheric oscillations in neutral wind, density, and pressure that propagate zonally and also vertically from their sources in the tropospheric-stratospheric regions. They have periodicity varying from 2 to 20 days and propagate globally, mostly westward, with significant meridional and zonal velocity components (e.g., Forbes 1996). They have zonal wave length of several thousands of kilometers, with small vertical wave length (of a few tens of kilometers), which limits their upward propagation to middle atmosphere and lower thermosphere and perhaps up to the dynamo region. Kelvin waves are one type of PWs (generated in the troposphere) that are trapped in the equatorial region and propagate eastward (e.g., Salby and Garcia 1987; Liu et al. 2012). The ultra-fast Kelvin (UFK) wave that has a period of 3–4 days and vertical wave length of 30–50 km is of particular interest to us since it can propagate upward to even higher altitude into the thermosphere with significant amplitude dominated by zonal wind component. The atmospheric tides, especially the diurnal and semidiurnal waves (due to their larger vertical wave lengths), reach ionospheric heights where they produce dynamo electric fields that drive the regular ionospheric dynamics including the current systems and the plasma drifts. Nonlinear interaction can occur between planetary/UFK waves and tidal waves (Pancheva et al. 2003), and the resulting modulated tidal winds interacting with the dynamo region is believed to control the PRE vertical drift and F layer height variations (Abdu et al. 2015a). The variabilities

in these driving sources when they are imposed on the "modifying parameters" mentioned above constitute the basic drivers of the day-to-day and short-term variabilities in the development and occurrence of the EPB/EFS irregularities.

The main paths by which the short-term variability in the EPB can occur are through changes in the following parameters: (1) The PRE vertical drift that mainly controls the linear growth rate. It can undergo large variations through superposition of vertical drifts due to disturbance electric fields, in the form of prompt penetration electric field (PPEF) and disturbance wind dynamo electric field (DDEF), when they occur in the evening hours. The PRE can undergo changes also through planetary/Kelvin wave modulation of the tides (as mentioned above) that modify the longitudinal gradient in the E layer Pedersen conductivity at sunset that controls the PRE. To understand this process better, we may consider, for example, the zonal component of a modulated tidal wind interacting with the E region plasma in the environment of large height gradient in the ratio of ion-neutral collision-to-gyro frequency. The zonal wind can cause vertical motion of ions (both the molecular and atomic ions) that may modify the E layer density, to different degrees, on the day- and nightside of the terminator. Thus, the evening time zonal wind can cause significant modification in the sunset longitudinal gradient in plasma density and hence in the E layer Pedersen conductivity. As indicated in Fig. 1, the PRE can be modified also by gravity waves induced oscillations in the evening F layer heights. (2) Variability in the seed perturbations in the form of precursor wave structure (with associated perturbations in polarization electric field), possibly induced by gravity waves, is another source of the short-term variability. When the PRE vertical drift has relatively smaller amplitudes, its modulation by gravity waves may also become significant as will be discussed later. (3) Meridional/trans-equatorial winds (U^{P}_{FT}) that can modify the field line integrated conductivity that controls the instability linear growth rate as well as the nonlinear growth of the plasma bubble. The (U^{P}_{FT}) arises from the north-south asymmetry in the thermospheric heating during quiet time (as also by the storm time asymmetric heating of the high latitude thermospheres). We will briefly discuss below some new and recent results on the short-term variabilities in EPB irregularities arising from the various sources mentioned above, highlighting their important characteristics and the electrodynamics conditions in which they occur.

EPB/ESF variability operating through changes in PRE

Observationally, the dependence of EPB/ESF development on the PRE vertical drift has been investigated extensively (e.g., Abdu et al. 1983, 2009c; Fejer et al. 1999; Huang and Hairston 2015). The PRE can suffer variability in two ways: (1) superposition of the vertical drift due to penetration electric field and disturbance dynamo electric field on the PRE which will be discussed in Section 2.1 and (2) changes in the two basic parameters responsible for its normal development mentioned earlier, that is, (a) the thermospheric zonal wind in the evening and (b) the longitudinal gradient in the E layer conductivity across the terminator. Item 2(a) will not be discussed specifically. Item 2(b) on conductivity gradient that involves the role of *E* layer winds (due to upward propagating atmospheric waves) will be discussed in Section 2.2. When the PRE is of weak intensity, it may suffer significant modification also due to gravity waves, which will be discussed in Section 3. We may further note that the PRE vertical drift is known to be part of the post-sunset plasma vortex flow, in which the E layer zonal wind has a contribution to the vertical shear in the zonal plasma, as studied using the thermosphere ionosphere electrodynamics - general circulation model (TIE-GCM) by Rodrigues et al. (2012). We will not be discussing here the specific role of this process in the PRE variability. Another question concerns the identification of threshold levels in the PRE vertical drift and in the associated post-sunset F layer height required for the EPB/ESF development. Such threshold levels can vary significantly depending upon the longitude, season, and solar flux conditions of the analyzed data (for more details see, for example, Farley et al. 1970; Abdu et al. 1983; Fejer et al. 1999; Manju et al. 2007; Smith et al. 2016). It should be kept in mind that the degree of variability in the ESF occurrence, to result from a change in the PRE or from an imposed disturbance electric fields to be described below, should depend inevitably upon the threshold conditions for their development prevailing at the time of the occurrence of the disturbances.

Short-term variability in PRE due to penetration electric fields and disturbance dynamo electric field

The magnetospheric electric fields penetrating to low and equatorial latitudes under disturbed conditions can cause drastic modifications in the ionospheric currents and plasma structuring (see, for example, Nishida 1971; Kikuchi et al. 1996; Basu et al. 2001; Fejer 2011; Abdu et al. 2003; Abdu 2012). Under the interplanetary magnetic field (IMF), Bz, southward conditions and the reconnection process the interplanetary electric field maps to high latitudes. The energy transfer process that follows is responsible for the rapid auroral electrojet intensification marking a substorm development, which may often be accompanied by concurrent global storm development manifested by rapid ring current intensification indicated by Dst decrease. The high latitude electric field, identified also as magnetospheric convection electric

field, promptly penetrates to equatorial latitudes as an under-shielding (dawn-dusk) prompt penetration electric field (PPEF) that has eastward polarity in the dayside-evening sector and westward polarity in the night sector (Fejer and Scherliess 1995; Kikuchi and Hashimoto 2016). A shielding layer due to the region-2 FAC (field aligned current) develops in time scale of 20–30 min to balance the convection electric field so that a subsequent northward turning of the Bz marking an auroral electrojet (AE) recovery may result in equatorward penetration of an over-shielding electric field (OSEF). The OSEF polarity is dusk-to-dawn, (opposite to that of the PPEF), that is, westward in the dayside-evening sector and eastward in the night sector (Kelley et al. 1979; Fejer et al. 2008). The OSEF is typically followed by disturbance wind dynamo (arising from auroral heating) with the associated electric field (DDEF) dominating the equatorial latitudes. The DDEF becomes active with a time delay of a few hours (3–4 h) from the storm development, often coinciding with the recovery phase of the storm (Blanc and Richmond 1980; Richmond et al. 2003). The polarity of the penetration electric field in the sunset sector, with its associated vertical drift complementing the PRE vertical drift, is a very crucial factor for the post-sunset EPB development (Abdu et al. 2003, 2009b; Li et al. 2010). An example of the contrasting effects due to under-shielding and over-shielding electric fields occurring in the evening over Fortaleza (3.9° S, 38.45° W, dip angle − 9°), Brazil, is presented in Fig. 2 (Abdu et al. 2009b, see also Abdu et al. 2012). On 25 September, the Bz turning south (with weak amplitude) at ~ 1930 UT (LT = UT−2 h 28 min at Fortaleza) initiated an AE activity, also of weak amplitude, that soon intensified at ~ 20:30 (~ 1800 LT) marking a substorm. At this time, the PRE was already under development over Fortaleza longitude. The under-shielding PPEF of eastward polarity associated with the AE intensifications and the (eventual) substorm development caused an enhancement in the evening vertical drift that was superposed on PRE vertical drift. The PRE vertical drift so enhanced attained a peak value of ~ 75 m/s at 21:30 UT (1902 LT) as compared to the 50 m/s peak drift of the quiet time PRE (shown in blue curve, bottom panel) that usually occurs at ~ 22:00 UT (19:32 LT). The large enhancement in the PRE vertical drift due to the PPEF caused prompt development of EPB (indicated by vertical pink bars) half hour earlier than its typical quiet time onset. In contrast to this, on 23 September, the Bz was southward with the AE activity (and the Dst decrease not shown here) prevailing several hours prior to the evening. The subsequent Bz turning north at 19:40 UT (17:12 LT) caused a rapid recovery in the AE activity that approached zero by ~ 21 UT/18:32 LT, (panel 3). The associated over-shielding electric field of westward polarity appears to be largely responsible for the near total suppression of the PRE on this evening (green curve in bottom panel). In view of the disturbance condition prevailing several hours (at least 6 h) prior to sunset, the role of a DDEF of westward polarity may also have contributed to this PRE suppression, as a result of which the usual post-sunset EPB did not develop on this evening.

Regarding the PRE enhancement due to under-shielding PPEF, we note that its intensity could depend upon the strength of the penetration electric fields as illustrated by the example of an event sequence presented in Fig. 3 (Abdu et al. 2018). On 16 September, the Bz southward fluctuations were present starting from ~ 10 UT, which was followed by an AE intensification (still under Bz south condition) starting at ~ 21 UT (18 LT) that coincided with PRE development time over Sao Luis (2.33° S, 44.2° W, dip angle −.5°) (SL). A PPEF of eastward polarity associated with the AE intensification appears to have caused an increase in F layer heights plotted at sequential plasma frequencies (panel 3) as well as in the enhanced PRE vertical drift that peaked at ~ 60 m/s over Sao Luis (bottom panel). The quiet day value of the peak PRE vertical drift was about 27 m/s (red curve), which is normally below the threshold value required for ESF development in September. The enhancement in the PRE vertical drift on this evening corresponded to an eastward penetration electric field of 0.6 mV/m. As a result, ESF developed promptly over Sao Luis having onset at 21:30 UT (18:30 LT) (panel 3) followed by its delayed onset at 22:30 UT (19:30 LT) over Cachoeira Paulista (CP) (22.6° S, 315° E; dip angle: − 28°) (panel 4). The time delay of 60 min corresponds to the vertical growth time for the EPB observed over Cachoeira Paulista. Thus, the enhanced vertical drift due to an under-shielding PPEF of eastward polarity appears indeed to be responsible for the EPB generation manifested in the form of the ESF development observed sequentially at SL and CP. The approximate bubble rise velocity in this case may be estimated as 150 m/s. A more intense disturbance activity marked the evening of 17 September when a large Bz southward turning, accompanied by a large AE intensification, which occurred at ~ 20:00 UT. The Dst decrease starting at this time (not shown here) dipped to − 180 nT at 23:30 UT marking an intense storm. The beginning of this storm disturbance at ~ 20 UT also coincided with the PRE development time as was the disturbance on the previous evening. The under-shielding PPEF of eastward polarity (associated with the storm) caused large enhancement in the vertical drift that was superposed on the PRE vertical drift, which peaked at ~ 100 m/s over SL near 22:00 UT/19:00 LT. The PPEF intensity in this case was estimated as 1.7 mV/m. This appears to have caused the prompt ESF development observed first over SL, followed by CP with a time delay of only 30 min. This time delay is much shorter than that was observed in the case of such sequential

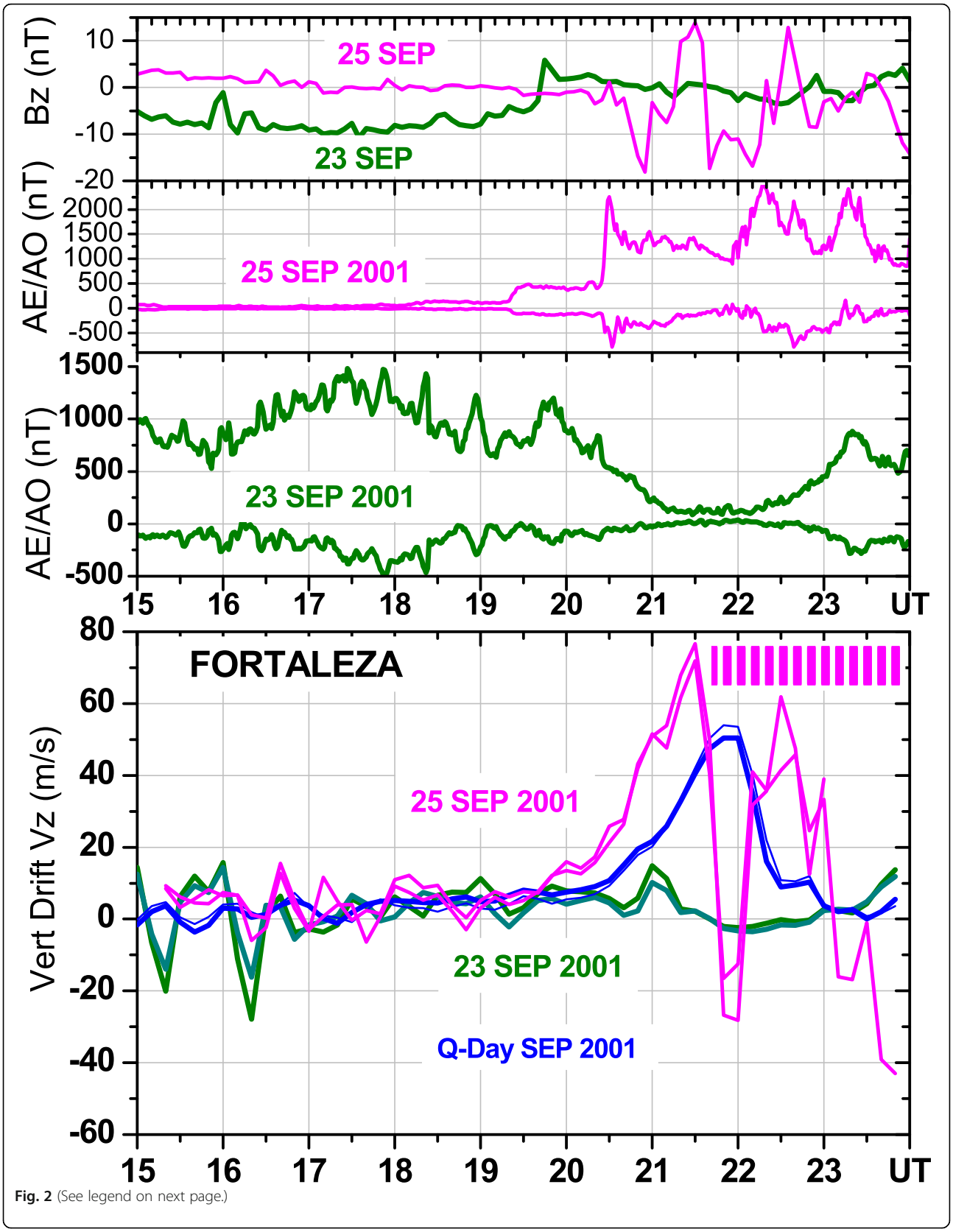

Fig. 2 (See legend on next page.)

(See figure on previous page.)
Fig. 2 Variations in the IMF Bz from ACE satellite on 23 and 25 September 2001 (green and pink curves, respectively) (top panel), auroral indices AE/AO for the same 2 days, from WDC Kyoto site (second and third panel), and vertical drift Vz (that is, d(hF)/dt) over Fortaleza (bottom panel). The Vz values were calculated at plasma frequencies 6 MHz and 7 MHz. They are shown for 23 and 25 September, respectively, in green and pink, together with a quiet day reference (in blue). The ESF occurrence staring at 2140 UT on 25 September is indicated by vertical bars

occurrence on the previous day which was 60 min. For this case of shorter time delay, the bubble rise velocity can be estimated as ~ 300 m/s. The SF is found to be of longer duration (and perhaps more intense as well) in this case than it was on the previous evening. These results clearly show that an under-shielding PPEF occurring during the evening (at the time of PRE development) may enhance the vertical drift due to the PRE, resulting in the generation of EPB. The larger the intensity of the PPEF the more intense will be the PRE vertical drift and the resulting EPB rise velocity (as judged from Digisonde observations). The increases in the intensity of the PRE and in EPB/ESF with increasing intensity of the penetration electric field as verified in these results might suggest an apparent proportionality in the observed cause-effect sequence. However, such a proportionality sequence does not seem to hold for abnormally large intensity of the disturbance electric field. For example, from analysis of radar and Digisonde data during the October 2003 magnetic super storm, Abdu et al. (2008a, 2008b) found that a large uplift of the F layer at a velocity approaching 1000 m/s over Brazil that was driven by an intense eastward electric field of ~ 30 mV/m did not produce any UHF (GPS) scintillation or enhanced spread F in ionogram. The observation was made in a region strongly influenced by the South Atlantic (or South American) Magnetic Anomaly (SAMA) wherein enhanced ionization by storm-induced energetic particle precipitation is believed to produce a large-scale gradient in the E layer conductivity that could be responsible for the development of polarization electric field superposed on the primary PPEF. It was intriguing, however, that the resulting abnormally large electric field did not support instability growth at the bottom side of the very rapidly rising F layer. Under normal conditions, the bubble rise velocity as modeled by the R-T mechanism is of the order of 200 m/s (e.g., Zalesak et al. 1982). ALTAIR observation showed a rise velocity of the order of 130 m/s (as inferred from Fig. 5 of the paper by Tsunoda 2015). It is not clear to what degree this rise in velocity may increase through modification of the instability growth parameters by the effect of an additional disturbance penetration eastward electric field occurring in the post-sunset hours. It needs to be investigated by detailed modeling studies. For the present discussion, we believe that the abnormally large intensity of the PPEF caused an F layer uplift at a rate (~ 1000 m/s) that was significantly higher than an instability vertical growth rate (rise velocity) possibly attainable under the R-T instability control parameters (see Eq. 1) that were also modified by the same strong PPEF. It is likely that the large uplift of the layer might have caused a large increase in the bottom side gradient length parameter L_{FT} that could cause a decrease in the growth rate to a larger degree than an increase in it that could occur by corresponding increases in the other terms (of Eq. 1). It appears that such a situation could be a key factor in causing the breakdown of the R- T instability growth process under the extreme situation that existed. As a result, an enhanced development of EPB did not occur on this night. It is not clear what should be the limiting value of the F layer uplift rate at which the EPB instability growth by R-T mechanism may become inoperative as we normally understand the process.

As regards the PRE vertical drift suppression by an over-shielding westward electric field, it is possible to identify the unique role of this electric field in specific cases without the possibility of concurrent contributions to them arising from the DDEF that also has westward polarity in the evening. For this purpose, it is necessary to consider cases of AE activity decay phase (normally indicative of northward turning of the IMF Bz) occurring just prior to sunset hours that are preceded by weak, or insignificant, Dst decrease so that the westward electric field occurring at sunset could be dominantly, if not exclusively, due to over-shielding conditions. The result of a statistical analysis of 18 cases of AE decay prior to sunset that occurred during the period of October to December 2003 is presented in Fig. 4. The Sym-H/Dst index variation shown in the top panel of the figure represents the mean of its superposed variations corresponding to all the cases of AE variations that presented decay in activity just preceding the evening PRE development. The corresponding mean AE variation is shown in the middle panel. The mean of the Vz variations for the same group of days (pink curve) is compared with that of the 10 quietest days of the same period (blue curve) in the bottom panel. The comparison shows a significant suppression in the PRE vertical drift due to the over-shielding westward electric field associated with the rapid AE decay/recovery that just preceded the sunset (that is, the PRE vertical drift). The quiet day PRE vertical drift peaked at 35 m/s, and the PRE decreased to 20 m/s as a result of the AE decay that just preceded it. The weak intensity of the Dst variations that characterized the sampled days, especially during several hours prior to sunset, may clearly rule out the possibility of any DDEF effect, also of westward polarity, influencing the PRE suppression

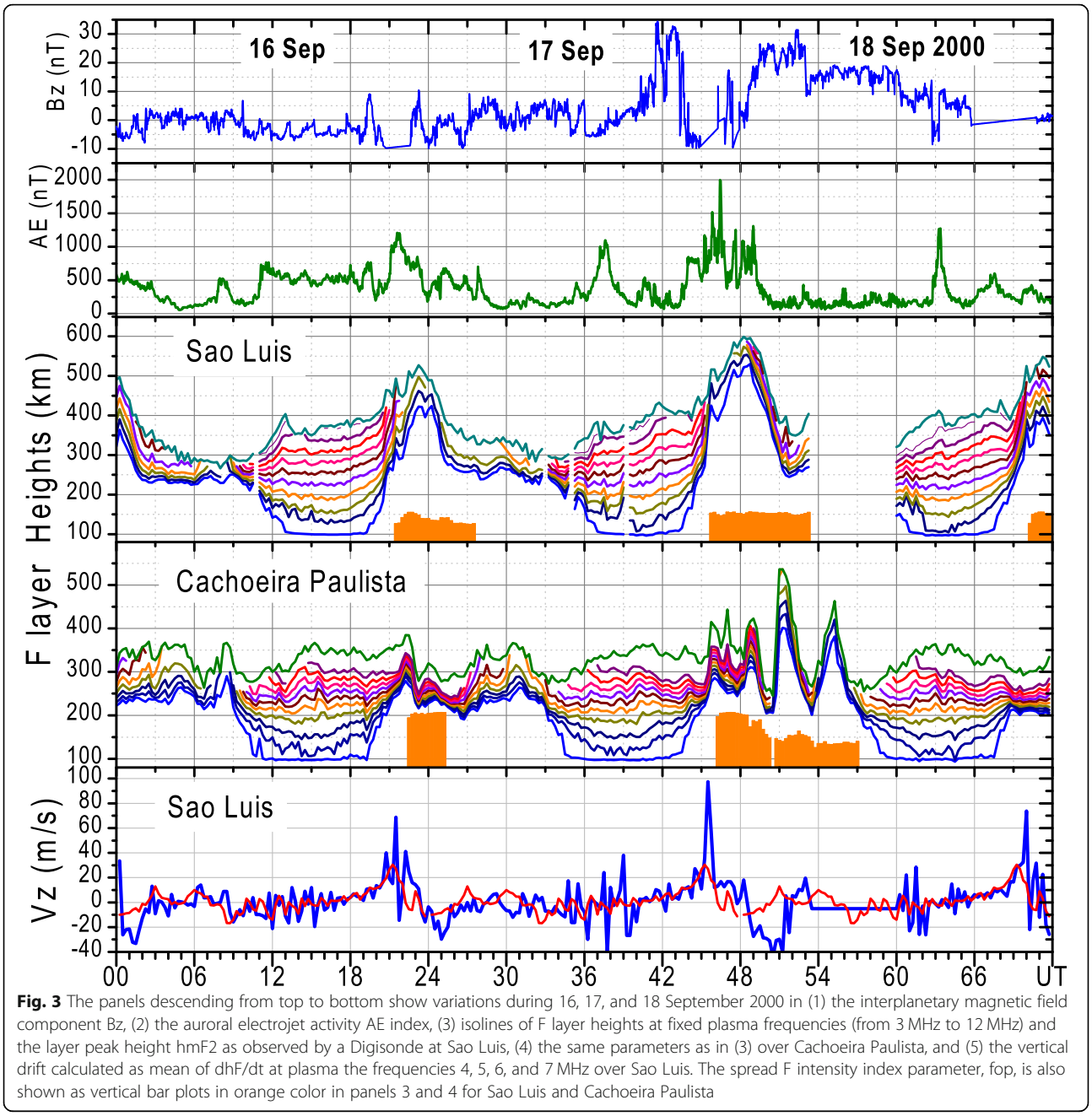

Fig. 3 The panels descending from top to bottom show variations during 16, 17, and 18 September 2000 in (1) the interplanetary magnetic field component Bz, (2) the auroral electrojet activity AE index, (3) isolines of F layer heights at fixed plasma frequencies (from 3 MHz to 12 MHz) and the layer peak height hmF2 as observed by a Digisonde at Sao Luis, (4) the same parameters as in (3) over Cachoeira Paulista, and (5) the vertical drift calculated as mean of dhF/dt at plasma the frequencies 4, 5, 6, and 7 MHz over Sao Luis. The spread F intensity index parameter, fop, is also shown as vertical bar plots in orange color in panels 3 and 4 for Sao Luis and Cachoeira Paulista

effect attributed to the over-shielding westward electric field. The weakened PRE vertical drift caused correspondingly weakened EPB development on the different days studied (not shown here).

In a typical sequence of magnetic disturbance phases the disturbance dynamo electric field occurs with a delay of a few hours (usually 4–5 h) from the onset of the storm disturbance (Sastri 1988; Fejer and Scherliess 1995; Scherliess and Fejer 1997). In the case of a clear/isolated substorm event, the DDEF if present should be easily observable within a few hours after the over-shielding electric field. During a typical global storm event characterized by a significant Dst decrease, the DDEF should be observable during the Dst recovery phase. The DDEF, with its westward polarity in the evening, may cause reduction in the PRE vertical drift leading to suppression of the post-sunset EPB development (as mentioned before). At later hours, its eastward polarity produces upward drift (layer rise), which may result in EPB development during post-midnight hours (Carter et al. 2016; Abdu 2012). Carter et al. (2016) analyzed scintillation data from GPS and VHF receivers, and ionosonde data, covering a wide

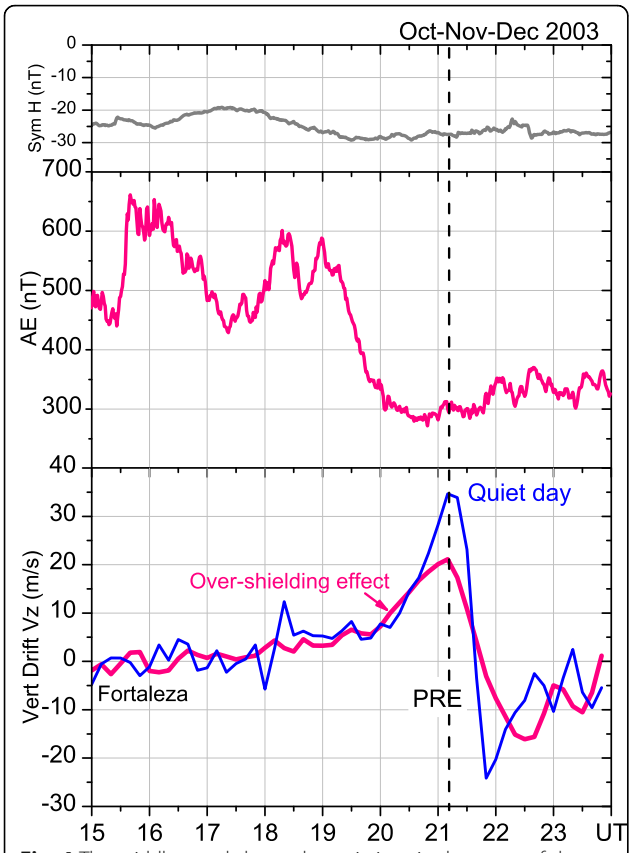

Fig. 4 The middle panel shows the variations in the mean of the superposed values of 18 cases (on 18 days) of AE decay that occurred just prior to sunset during the period October, November, and December 2003. The top panel shows the corresponding mean variation in the Sym-H/Dst values, and the bottom panel shows the corresponding variation in the vertical drift velocity (pink curve) and the mean of ten quiet days of vertical drift (blue curve), demonstrating the PRE vertical drift suppression due to over-shielding westward electric field

range of longitude, during the 17 March 2015 storm. Calculation of the Rayleigh-Taylor linear growth rate based on coupled thermosphere –ionosphere modeling (TIE-GCM) results during an event sequence showed that post-sunset inhibition, or post-midnight development, of scintillation could be caused by disturbance dynamo electric field contributing, respectively, to decrease or increase the instability growth rate.

Short-term variability through PRE modifications by atmospheric waves

The PRE vertical drift and post-sunset F layer heights can be modified significantly by upward propagating atmospheric waves originating from the sources of their generation in the lower atmosphere. These waves are, as mentioned before, the gravity waves, planetary/Kelvin waves and tidal waves. The results of such modifications constitute an important component of the ESF/EPB variability to be considered under magnetically quiet conditions. The planetary- and Kelvin- waves (especially the ultra-fast Kelvin waves; UFK) of 3–5 days of periodicity in their upward propagation have been observed to produce oscillations in the PRE vertical drifts (Abdu et al. 2006a, 2015a) and in post-sunset equatorial F layer heights (see, for example, Takahashi et al. 2006, 2007; Fagundes et al. 2009). Manifestations of these waves in the post-sunset F region have been established through studies comparing the oscillations characteristics of mesospheric winds with concurrent oscillations in the evening PRE vertical drift and post-sunset F layer heights. Good correlation was found between the 3–5 day periodicity in the mesospheric zonal wind over a low-latitude station, Cachoeira Paulista (22.6° S, 315° E), and the PRE vertical drift over an equatorial site, Cachimbo (9.46° S, 54.83° W), as demonstrated by Abdu et al. (2006a). Takahashi et al. (2006) showed that the planetary wave oscillations at 3–6 day period in mesospheric zonal wind (near 90 km) over the equatorial sites, Cariri (7.4° S, 36.5° W) and Ascension Island (7.9° S, 14.4° W), were well correlated with such oscillations in the post-sunset F layer heights (h'F) at 20:00 LT over Fortaleza (3.9° S, 38.4° W, Geomag. 2.1° S). Takahashi et al. (2007) found also 3–4 day oscillations in the meteor radar zonal wind over Cariri and in foF2 and h'F at 20:00 LT over Fortaleza correlating with the upward propagating TIMED/SABER temperature wave of the same period, which suggested the process of UFK wave modulation of the equatorial nighttime ionosphere. The above results may point to the presence of planetary/UFK wave-induced variability also in the ESF/EPB irregularity development that are basically controlled by the PRE vertical drift or the post-sunset F layer heights that are modified by these waves. Modulation of the PRE vertical drift, accompanied by corresponding modulation in the post-sunset ESF development, by UFK and FK waves was demonstrated by Abdu et al. (2015a). As an example, Fig. 5 shows a wavelet spectrum of the PRE vertical drift (bottom panel) with corresponding variations in ESF intensity (top panel) in response to a UFK wave episode that occurred in October 2005 as corroborated from observations of upward propagating temperature wave (seen in TIMED/SABER data) and mesospheric winds over Tirunelveli (8.7° N, 77.8° E) and Cariri (not shown here, but see Abdu et al. 2015a). We may note that increases in PRE vertical drift (such as those indicated by vertical arrows in the middle panel) due to the 3–4-day UFK wave were responsible for the earlier onset and higher intensity of the spread F on these days. As explained in Abdu et al. (2015a), the peak UFK wave activity at mesospheric heights occurred some 10 days earlier to its manifestation as PRE vertical drift at the F layer heights. From this time delay in the PRE vertical drift (with respect to the UFK activity at mesospheric

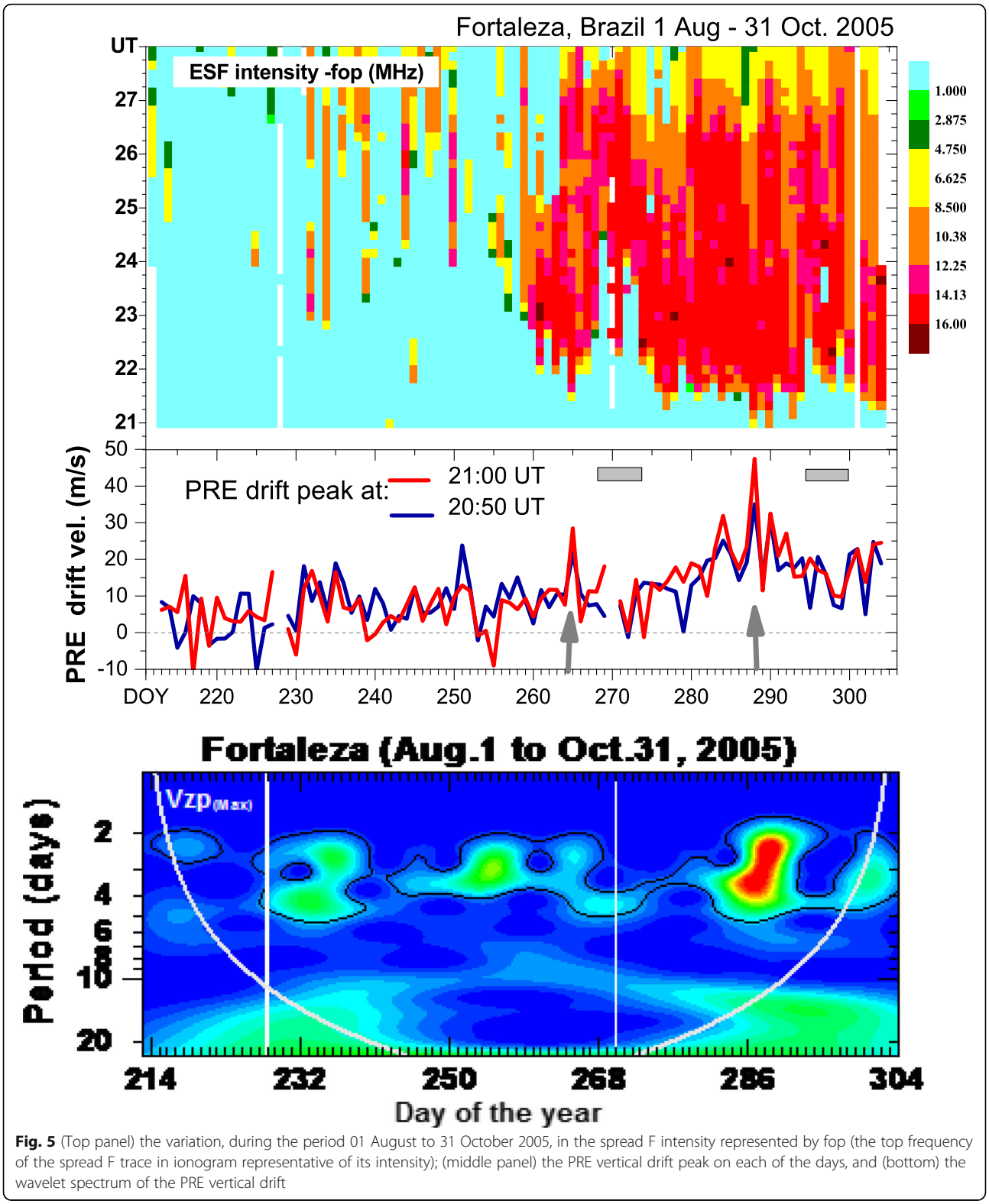

Fig. 5 (Top panel) the variation, during the period 01 August to 31 October 2005, in the spread F intensity represented by fop (the top frequency of the spread F trace in ionogram representative of its intensity); (middle panel) the PRE vertical drift peak on each of the days, and (bottom) the wavelet spectrum of the PRE vertical drift

heights), the vertical propagation velocity of the UFK waves was estimated as ~ 5 km/day, which is in agreement with previous results (e.g., Pancheva et al. 2003). In this way, it was possible to conclude that the waves propagating up to the dynamo region (~ 140 km) was responsible for the effects observed in the F region in the form of the PRE vertical drift and ESF development. Such PRE vertical drift modulation is possible through

a corresponding modulation of the longitudinal/local time gradient in the E layer conductivity around sunset that may be shaped by the E layer zonal wind (Abdu et al. 2006a). As explained by Abdu et al. (2006a), the tidal modes of the E layer winds could be modified by nonlinear interaction with upward propagating UFK waves (similar to the cases of planetary wave modulation of the tides through nonlinear interaction as explained by Pancheva et al. 2003). The E layer winds so modified could in turn cause changes in the longitudinal gradient in E layer conductivity (as was explained in Section 1.1), which could lead to the PRE modulation by the UFK waves (Abdu et al. 2006a; Abdu and Brum 2009). This cause-effect sequence highlights the important role of E layer winds in causing the variabilities in PRE and ESF/EPB developments, a point we will be discussing again. It is relevant to point out in this context that the ability by the TIE-GCM to predict realistic PRE vertical drift depended on the adjustments in the night E region density and in the amplitude and phase of atmospheric tides (Fesen et al. 2000).

We may note here that the upward propagating waves in the form of tidal modes and planetary/Kelvin waves are of global scale and therefore their modulation of the PRE vertical drift and ESF may not present any perceivable zonal (longitude) variation as such. In contrast to this, the typical gravity wave scales are of the order of a few hundred kilometers. For example, the large-scale wave structure (LSWS) in which the EPB seeding may take place, and which can also be associated with (or identified as) the seeding gravity waves, have local scales of the order of a few hundreds of kilometers, typically 400–600 km, (e.g. Tsunoda and White 1981), which may suffer significant zonal variation depending upon the locations of the wave generation source. As a result, we may expect significant zonal variation in the EPB seeding process due to gravity waves, whereas such zonal variation due to the modulation effects by tidal and planetary/Kelvin waves appears to be absent.

Gravity waves and EFS/EPB variability

An instability seed perturbation is an important requirement for initiating the EPB development although its diagnostics based on observational data has been a challenging task. Gravity waves originating from sources in lower atmosphere were invoked to explain the spatial structures observed in HF radar maps of the ESF irregularities (Rottger 1981). On a statistical basis, the role of gravity waves in the longitudinal and seasonal distribution of spread F has been in part attributed to gravity wave generation at the inter-tropical convergence zone (ITCZ) and to its geographical and seasonal migration (McClure et al. 1998; Tsunoda 2010). From analyses of the seasonal/global distribution of plasma irregularities observed by the ROCSAT-1 and from the OLR/ITCZ data, Su et al. (2014) found that the role of gravity waves was recognizable mainly in South American and African longitude sectors, and not over all longitudes. More recently, from comparison of bubble irregularity occurrences at close-by locations in Asian sector, Li et al. (2016) found that enhanced plasma bubble generation was associated with more active ITCZ sector. On a case study basis, the role of gravity waves in seeding the ESF irregularities has been investigated for different longitude sectors (see, for example, Abdu et al. 2009a, Sreeja et al. 2009). Based on ionosonde and radar data, it was found that for smaller (larger) PRE vertical drift velocities a larger (smaller) amplitude of the gravity wave perturbations (in density and polarization electric field) was required to produce a given instability growth rate for the ESF development (Abdu et al. 2009a). In other words, an evaluation of the role of gravity waves (in the form of a precursor seed perturbation) in a given EPB irregularity development would also require a simultaneous assessment primarily of the prevailing PRE vertical drift amplitude and possibly other related parameters as well.

The precursor condition for ESF development has been identified also in the form of large-scale wave structures (LSWS) in the background electron density as observed by east-west scan incoherent scatter radar (Tsunoda and White 1981). It has been observed also in the form of longitudinal wave structures in the sub-ionospheric total electron content (TEC) as measured from C/NOFS satellite passes (for example, Thampi et al. 2009; Tsunoda et al. 2011) and Tulasi Ram et al. 2014). It may also appear as an additional F layer trace (satellite trace) in ionograms (e.g., Abdu et al. 2014; Tsunoda 2008; Li et al. 2012). These wave structures have scale sizes of a few hundreds of kilometers (400–800 km), and they are present in the F region well before sunset. They may resemble the wave structures represented by gravity wave-induced F layer height oscillations analyzed by Abdu et al. 2009a. Statistically, their amplitude may grow towards sunset and can be maintained by polarization electric field whose sustenance under daytime/afternoon conditions and amplification towards sunset have been explained by Abdu et al. (2015b). These features are illustrated in Fig. 6, which shows two sets of examples presented for two solar activity maximum epochs: (a) October–December 2002 (F10.7: 170) and (b) October 2014 (F10.7: 155). Figure 6a shows in the upper two panels the F layer height oscillations in the period range 0.5–1.5 h, as superposed plots, for two groups of days of the epoch (a) that include a total of 66 days of observations. In one group, we may note oscillations that appear nearly in-phase (coherent) on all days, with the amplitude increasing towards sunset, and transitioning into larger amplitudes corresponding to post-sunset spread F indicated by the gray segment of the

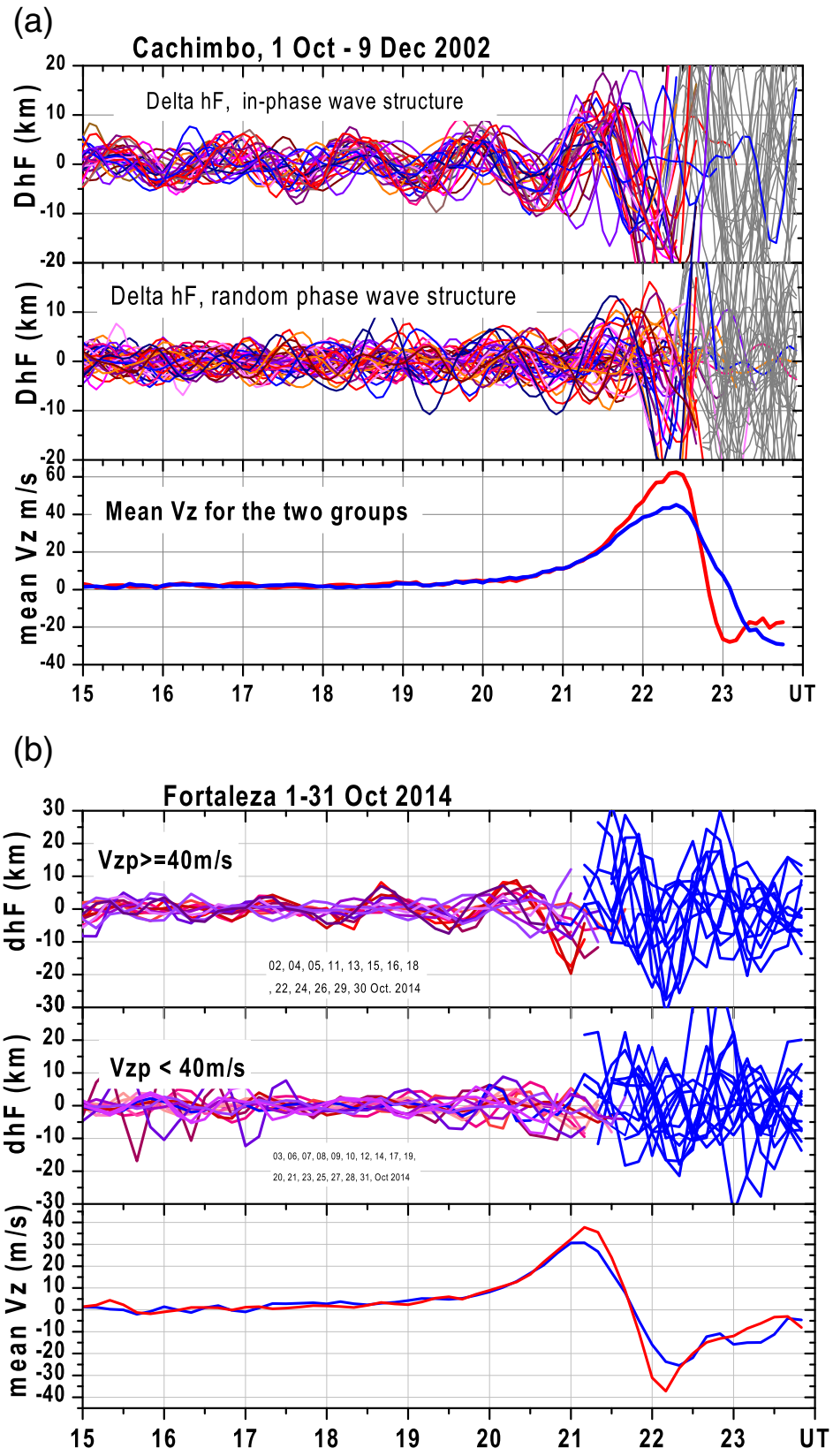

Fig. 6 (See legend on next page.)

(See figure on previous page.)
Fig. 6 a Top panel: F layer height oscillations at 8-MHz plasma frequency obtained by band-pass filtering (0.5–1.5 h period) of the true height measured at 5 and 7.5-min cadence by a Digisonde at Cachimbo, Brazil. The superposed oscillations for a selected set of days (from a 66-day period) are nearly in-phase (coherent) on all days. Middle panel: Similar plots for the group of remaining days of the 66-day period that show the oscillations mostly in random phase. The gray segment of each curve in both panels shows transition to spread F activity after sunset, with non-spread F hours continuing colored. Bottom panel: The mean of vertical drifts calculated as Vz = dhF/dt separately for the above two groups of days. (These data are from the COPEX Campaign, Abdu et al. 2009c at Cachimbo, LT = UT−3 h 40 min.) **b** Similar results as in Fig. 6a, but for the period of 1–31 October 2008 over Fortaleza, where LT = UT−2 h 32 min

curves (top panel). The other group (middle panel) shows nearly random phase (non "coherent") oscillations that also present amplification towards sunset (to a smaller degree than in the top panel) and evolve into spread F on most of the days. These results clearly demonstrate the presence of precursor seed perturbations that evolve into post-sunset ESF development. The precise nature of the competing roles of these precursor oscillations vis-à-vis the amplitude of the PRE vertical drift required for any specific ESF development has not been evaluated in these groups (as was evaluated in the case studies presented in Abdu et al. 2009a). The vertical drift on individual days was calculated as dhF/dt using the procedure described by Abdu et al. (1983). The variations in the mean vertical drift for the two groups are plotted in the bottom panel, which show that the peak of the PRE vertical drift for the first group of days (red curve) is significantly larger (by about 18 m/s) than for the second group of days (blue curve). In other words, the days of "coherence" in the gravity wave-induced F layer height oscillation during the afternoon pre-sunset hours corresponds to the same set of days during which the PRE vertical drift is larger than on the days of smaller height oscillations that are in "random phase" (lack of coherence). Similar relationship appears to hold also during the epoch (b) of solar maximum (plotted in Fig. 6b). In this case, however, the data sample is smaller (31 days only) and the PRE vertical drift velocities are also generally smaller than during the epoch (a). We may note that the day groups with "coherence" and "non coherence" in oscillations are apparent in this sample as well (but to a smaller degree). The difference between the PRE vertical drift velocity peaks in the two groups of days during this epoch is about 8 m/s only. It should be pointed out here that the grouping was based on whether the PRE vertical drift peak values were < 40 m/s or > 40 m/s, but possible displacements in the vertical drift peak times on different days must have caused some reduction/smearing in the mean values of the drift peak calculated at fixed local times. The amplification of the oscillation amplitude towards sunset evolving into spread F development is clearly brought out even though the "coherence" characteristics of the oscillations is less conspicuous in this case (of smaller group of days) than it was during the previous solar maximum epoch. What appears to be an apparent connection between the PRE vertical drift and the oscillation wave structure might indicate a possible interaction between the upward propagating gravity waves and the tidal modes of winds (as was suggested by Abdu et al. 2015b) since it is known that the tidal winds in the E layer could modify the E layer conductivity longitudinal gradient that controls the PRE development (Abdu et al. 2006a).

When the PRE vertical drift is relatively weaker, its peak value may suffer modification (even becoming further suppressed) by a gravity waves of strong enough amplitude depending upon its propagation phase. As a result, the post-sunset ESF may become weaker, delayed in development, or even suffer total suppression. Figure 7 shows (in top panel) the F layer height variations at sequential plasma frequencies, ranging from 3 MHz up to 12 MHz, (recorded by a Digisonde at Fortaleza) during a 3-day period in October 2008, an epoch of the extended solar minimum of the cycle 23. On 10 October, a very quiet day, the evening PRE vertical drift (second panel) peaked around 12 m/s (typical for this epoch), which is normally below the threshold value for ESF development, but spread F developed by 20:15 LT (as indicated in panel 3). We may point out here that the ESF development under such low PRE vertical drift could be occurring due to a relatively large amplitude of the gravity wave seed perturbation and/or very likely also due to an enhanced bottom side gradient (this aspect will be the subject of a separate study). Considering the evening of 12 October, which followed a moderate degree of magnetic disturbances as indicated by the AE variations (accompanied by a weak storm with Dst peaking at − 65 nT at 11:30 UT on 11 October, not shown here), the PRE vertical drift was ~ 15 m/s and range spread F developed at 19:15 LT. In this case, a slight enhancement in the PRE vertical drift (compared to that of 10 October) may be noticed. The enhancement appears to be caused by a penetration electric field of eastward polarity and of relatively weak intensity associated with a rapid AE intensification (see panel 4, Fig. 7) that occurred right at the time of the PRE (18 LT) (see panel 2) also indicated by a dashed vertical line. Spread F onset in this case was at 19:45 LT, earlier in LT than on 10 October (a quiet day) when the onset was at 20:15 LT. In contrast to these two cases (of 10 and 12 October), the PRE vertical drift reached negative values on the evening of 11 October

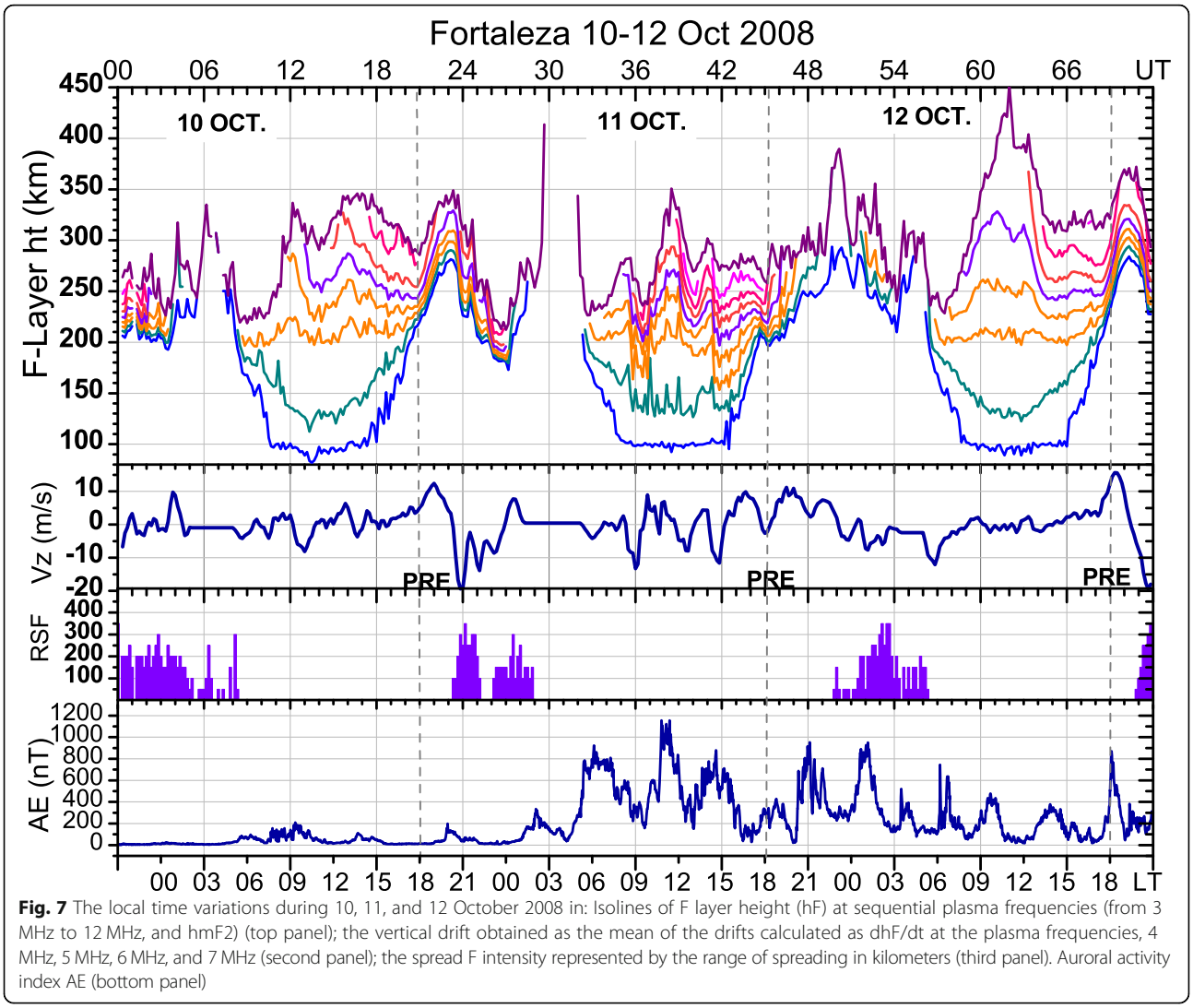

Fig. 7 The local time variations during 10, 11, and 12 October 2008 in: Isolines of F layer height (hF) at sequential plasma frequencies (from 3 MHz to 12 MHz, and hmF2) (top panel); the vertical drift obtained as the mean of the drifts calculated as dhF/dt at the plasma frequencies, 4 MHz, 5 MHz, 6 MHz, and 7 MHz (second panel); the spread F intensity represented by the range of spreading in kilometers (third panel). Auroral activity index AE (bottom panel)

when the observed peak drift was approximately – 3 m/s. But the real drift must be more negative than this if a correction is applied for recombination effect, which is not done, since we are comparing here only the relative behavior during these days. The post-sunset SF did not develop as a result, but SF did develop near midnight (around 23 LT), which may be related to the F layer height increase due likely to the AE activity that intensified around this time. An important point to note about this evening is that the suppression/reversal of the PRE vertical drift did not result from the magnetic disturbance that was present at this time as can be verified from the fact that the phase of the Vz variation did not conform to that of AE variation. (For example, the AE activity decreased from 15 LT to 17 LT when the F layer heights and the Vz increased contrary to their expected response, which is predicted to be a decrease in their values due to the over-shielding westward electric field expected to be associated with the AE decrease at this time.) The only clear case of an F layer height response to the AE activity on this day can be noticed near 11 LT (14 UT) when the height reached a peak value in association with the AE intensification that occurred at this time. The small decrease in the heights of the plasma frequency isolines around 18 LT (indicated by a dashed vertical line on 11 October) cannot be in response to the AE activity that was on a minor rising trend during this period (17–19 LT). A careful examination of the F layer height variation around 18 LT reveals the presence of a downward phase propagation in its oscillations, which is a clear signature of an upward propagating gravity wave. We are therefore led to conclude that the PRE suppression/reversal on this evening was the result of a gravity wave activity, which thereby leads to the stability of the post-sunset F layer. This is perhaps the first observation of a case in which a gravity wave activity apparently acted to suppress the ESF development which was otherwise favored by the existing background conditions (detailed

quantitative evaluation of this effect will be the topic of separate paper).

Variability in ESF due to disturbance trans-equatorial winds

The role of trans-equatorial (or meridional) winds in ESF/EPB development operates through the effect of these winds in modifying the field line integrated conductivity and the F layer bottom side gradient, as was shown from model study by Maruyama (1988). The ratio of the F region—to the total—field line-integrated conductivity should control the instability linear growth rate as represented by the Eq. 1. Further, a trans-equatorial wind (TEW) lifts up the F layer on the upwind side of the magnetic equator while bringing it down on the downwind side thereby producing correspondingly opposing (but unequal) effects on the bottomside density gradients. The field line perpendicular (meridional) components of the TEW on either sides of the equator are also in opposite directions. The net result is that the ratio U_{FT}^{P}/L_{FT} always contributes negatively to Eq. 1 thereby causing a decrease in the net growth rate. The consequence of such reduction in the growth rate has been invoked by Su et al. (2017) to explain the longitude-dependent solstice minimum in post-midnight irregularity occurrence observed in ROCSAT-1 data. Additionally, while a TEW may cause an increase in the field line-integrated conductivity (Σ_P) on the upwind side (where the layer is raised), it may cause decrease in Σ_P on the downwind side where the layer is lowered. But the latter effect is stronger than the former due to the height-dependent molecular ion composition, so that a net increase can occur in the total (field line integrated) value of Σ_P (Maruyama 1988). As a result, the nonlinear growth of the bubble to topside ionosphere can be retarded or even suppressed. Observational results corroborating the effect of TEW in suppressing the ESF/EPB growth during quiet time have been presented by, e.g., Abdu et al. (2006b), Maruyama et al. (2009), and Su et al. (2017). While the TEW can be more intense during the solstice seasons under quiet conditions, it can become intensified any time of the year during magnetic storm disturbances occurring under conditions of hemispheric asymmetry in auroral heating. We present below an interesting case of ESF suppression due to storm time TEW as inferred from conjugate point observations of hmF2 by Digisondes in Brazil.

Figure 8 shows in the upper panel the variations in the F layer vertical drift velocity (Vz) at three plasma frequencies (6 MHz, 7 MHz, and 8 MHz) during the severe magnetic storm event of 17–18 March 2017 together with its variation on 16 March as a quiet time reference curve (shown in the second panel). The vertical drift was calculated as dhF/dt from Digisonde ionograms. The spread F occurrence during the period is also shown (plotted using the intensity parameter "fop"). The variations in the AE and Dst indices are shown in the bottom two panels. Following the storm onset at 06 UT (as per the AE index) on 17 March, a series of AE intensifications occurred when it was mostly daytime over Fortaleza. This was accompanied by the Dst decrease that suggested a major category storm development. A few episodes of vertical drift enhancements (and reversals) due to the storm-associated prompt penetration electric field of eastward (and westward) polarity occurred during this period. Two of the major episodes in Vz peaked at ~ 13 UT and ~ 18 UT. Further, we may note in these cases that the drift enhancements varied with the plasma frequency, being larger for higher plasma frequency, that is, higher reflection height. This feature appears to be due to the height-dependent photo-chemistry (the ion production and recombination rates decreasing to higher altitudes) dominating the daytime ionosphere, whereby the vertical gradient in electron density becomes shallower as the layer rises under the penetration electric field. The next Vz enhancement occurred near 21:00 UT (18:00 LT) that coincided with the PRE vertical drift (indicated by the vertical line "1"). The quiet time PRE vertical drift (that of 16 March in panel 2) had a peak value of ~ 18 m/s, and spread F occurred on the evening of 16 March and continued till the morning hours of 17 March (as can be noted in panel 3). A PPEF of eastward polarity associated with an AE intensification occurred around 21:00 UT (of 17 March) that caused a large increase in the PRE vertical drift, which peaked at 40 m/s (twice higher than that of the quiet day), but unexpectedly, spread F did not develop on this evening. Further, all the three plasma frequencies presented the same vertical drift at this time, thereby indicating that the F layer bottom side density gradient remained unaltered during the layer rise. This is an important feature to be noted because it shows that the density gradient ($1/L_{FT}$) did not contribute to any alteration in the R-T instability growth rate (as per in Eq. 1) that could occur during the layer rise. The large increase in Vz resulted in a large increase in the F layer height (not shown here) whereby the reduced ν_{in} could result in an enhanced contribution to the linear growth rate arising from the gravity term (g/ν_{in}) in Eq. 1. Thus, we note from Eq. 1 that increases in both the vertical drift (E/B) term and the gravity term, under the condition of an unchanging L_{FT}, should have contributed to increase the linear growth rate. However, spread F did not occur on this evening, which might suggest that other factors must be responsible for suppressing the development of the ESF. A possible decrease in the growth rate γ_{FT} arising from a decrease in

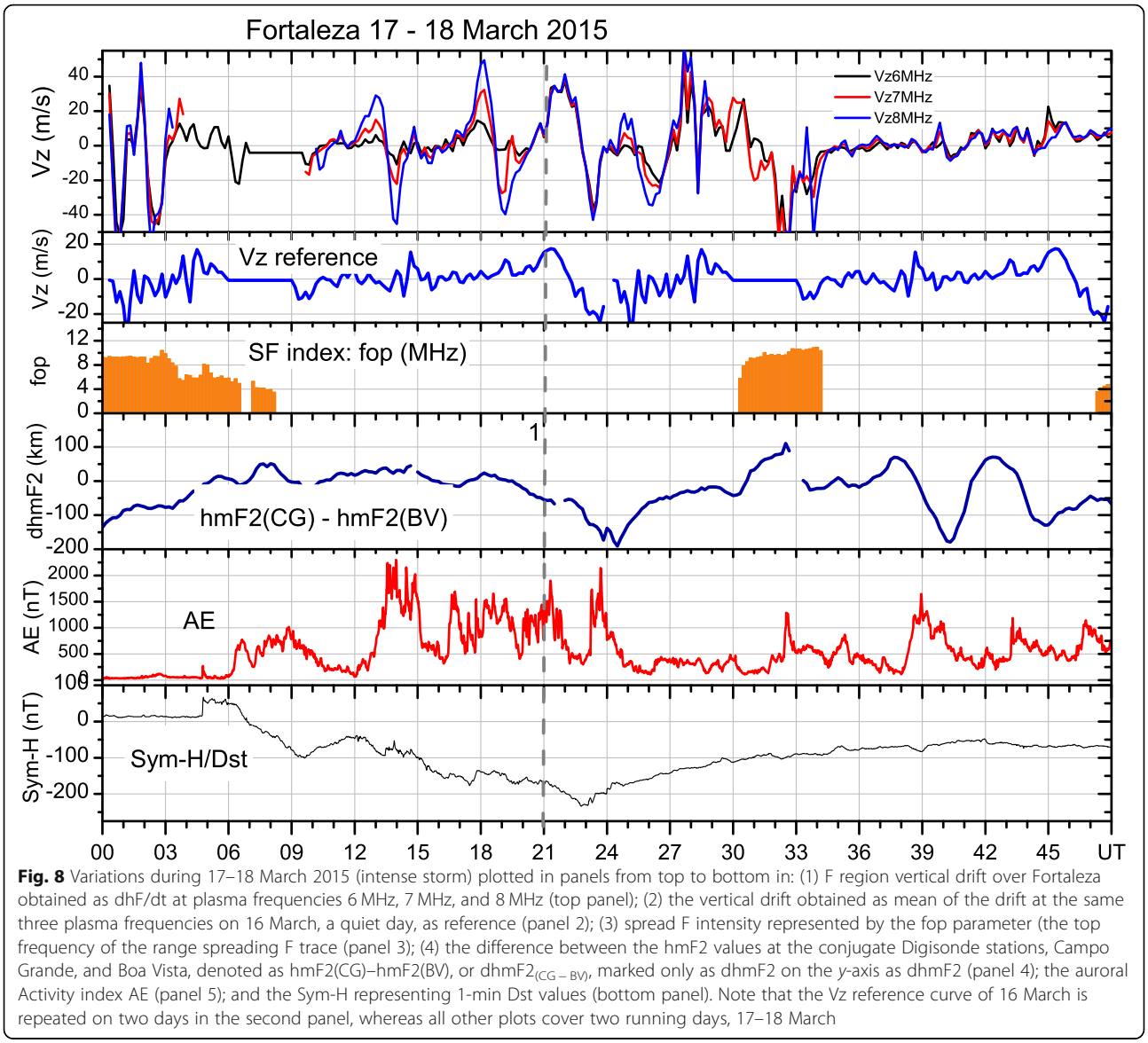

Fig. 8 Variations during 17–18 March 2015 (intense storm) plotted in panels from top to bottom in: (1) F region vertical drift over Fortaleza obtained as dhF/dt at plasma frequencies 6 MHz, 7 MHz, and 8 MHz (top panel); (2) the vertical drift obtained as mean of the drift at the same three plasma frequencies on 16 March, a quiet day, as reference (panel 2); (3) spread F intensity represented by the fop parameter (the top frequency of the range spreading F trace (panel 3); (4) the difference between the hmF2 values at the conjugate Digisonde stations, Campo Grande, and Boa Vista, denoted as hmF2(CG)–hmF2(BV), or $dhmF2_{(CG-BV)}$, marked only as dhmF2 on the *y*-axis as dhmF2 (panel 4); the auroral Activity index AE (panel 5); and the Sym-H representing 1-min Dst values (bottom panel). Note that the Vz reference curve of 16 March is repeated on two days in the second panel, whereas all other plots cover two running days, 17–18 March

the ratio of F region—to total—field line-integrated conductivity of the Eq. 1 is unlikely because there was no indication of any enhancement in the E region conductivity as may occur under disturbed conditions due to storm-associated enhancement in energetic particle precipitation, which can be assessed from Es layer data. No Es layer was present. Therefore, it looks possible to conclude that the only factor that could have caused a decrease in the growth rate on this evening must be that arising from the term in trans-equatorial/meridional wind in Eq. 1.

We examined the possible role of a TEW during this event by analyzing the hmF2 variations measured by the Digisondes operated at the conjugate sites, Campo Grande (Lat. − 20:26:34; Long. 54:38:47, dip − 22° 19′) and Boa Vista (Lat. 02:49:11; Long. 60:40:24, dip 22°), (see also Abdu et al. 2009c). We have used the variation in the parameter, $dhmF2_{(CG-BV)}$, obtained by subtracting the hmF2 over Boa Vista (BV) from that of Campo Grande (CG), to represent the variation in the TEW. It was shown by Abdu et al. (2009c), that a change of 1 km in this parameter corresponded to a change in TEW of ~ 1.5 m/s in the evening hours of our interest here. Panel 4 in Fig. 8 shows the variation in $dhmF2_{(CG-BV)}$ during 17 and 18 March 2015 (see also, Batista et al. 2017). Positive values in dhmF2 correspond to a TEW directed northward across the equator. We may note that on 17 March the dhmF2 that was mildly positive (for most of the time) turned negative starting at 18:00 UT (~ 14:30 LT) and remained so for the next few hours. This indicated that the TEW that was mostly northward turned southward to attain a value of around 90 m/s (corresponding to the $dhmF2_{(CG-BV)}$: − 60 km)

at 21:00 UT (~ 17:30 UT). We believe that this southward increase in the TEW could be responsible for decreasing the instability growth rate that caused the suppression of the ESF development, which otherwise was strongly favored by a PRE vertical drift that was enhanced by the disturbance eastward electric field. Numerical simulation of plasma bubble development was realized by Maruyama et al. (2009) in which trans-equatorial wind inferred from conjugate point ionosonde observations in Asian longitude (around 100° E) was incorporated. It was found that the growth time of the bubble increased by a factor two (meaning a slower growth) when the TEW velocity increased from 10 to 40 m/s. The result of Maruyama et al. (2009) corresponded to the conditions of quiet time equinoctial asymmetry in irregularity development. But it appears to be relevant to the present case of irregularity suppression under disturbed conditions as well, since the central question concerns the role of a TEW in effecting such suppression. In the present case, however, the TEW appears to require a relatively larger intensity due to the fact that the evening PRE vertical drift (accompanied by an additional vertical drift due to the PPEF) was larger (being twice that of its quiet time value) when the irregularity development was suppressed. Here, we have evoked the role of a TEW based on considerations of the terms in Eq. 1 that apply to linear growth phase of the R-T process. The role of a TEW to slow down the nonlinear growth towards suppressing the bubble vertical growth is not clear from this analysis, because there was no evolution to topside bubble to be monitored starting from an SF onset at the bottom side which did not occur to begin with.

Discussion

We have presented results above illustrating the different paths through which the short-term and day-to-day variabilities may occur in the development of the EPB/ESF irregularities. The range of time scales defining such variabilities was discussed in the introduction section. It is possible to consider the sources driving these variabilities as belonging to two broad categories (types): category 1: upward propagating atmospheric wave activity associated with tropospheric and/or stratospheric weather disturbances and category 2: magnetic activity that is typically associated with space weather disturbances. In both of the cases, different degrees of modifications are imposed on the specific parameters that are directly responsible for the instability growth leading to EPB/ESF development, as summarized below: (a) The PRE vertical drift (which perhaps is the most widely discussed parameter in the literature) that may suffer modification through (i) the penetrating magnetospheric electric field and the disturbance dynamo electric field as was described in Section 2.1 (category 2), (ii) the changes in E layer conductivity longitudinal gradient at sunset due to changes in tidal winds originating from PW/UFK wave modulation of the tides as discussed in Section 2.2, (category 1), and (iii) gravity wave modulation of the PRE vertical drift (when it is weak) as was described in the last paragraph of Section 3 (category 1); (b) the instability seed in the form of wave structure in density and polarization electric field, which is shaped by upward propagating gravity waves believed to be originating mostly from tropospheric convective activity associated with the ITCZ, as described in Section 3 (category 1); and (c) the total field line integrated conductivity of the E and F region as well as the ratio of the F region conductivity to the total field line integrated conductivity that can be modified by the TEW/meridional wind, during storm time (category 2) as well as under "quiet" conditions.

Regarding the item (a) above, we have shown that enhanced development, or suppression, of post-sunset EPB can arise from vertical drift velocity modifications that may occur under magnetic disturbances (in the form of sub-storm or storm) occurring right at the evening local time of the PRE development. When disturbances occur in the form of AE intensification under Bz south conditions, often accompanied by a Dst decrease indicating a storm development phase, the PRE vertical drift may become enhanced leading to EPB generation. The disturbance intensity may vary from that of a weak substorm to one of an intense storm, or may even be representative of an unidentifiable storm condition. It was shown that the PRE vertical drift as well as the associated plasma bubble rise velocity could increase with increase in the intensity of the under-shielding eastward PPEF. However, as was pointed out based on previous studies, an increase in the bubble rise velocity in a way proportional to the intensity of the PPEF will not be operative for abnormally large vertical drifts such as that may occur during some super storms. It was also discussed that while a DDEF of westward polarity in the evening hours may suppress the PRE vertical drift and, thereby, also the post-sunset bubble growth, such effects may also be produced by an over-shielding electric field of westward polarity associated with a substorm/storm recovery phase occurring just prior to sunset. Results of a statistical study based on a few cases of AE recovery phase occurring just prior to sunset hours clearly showed that the over-shielding westward electric field associated with such recovery phases could result in significant suppression of the PRE vertical drift, which may lead to a drastic decrease in EPB development, a detailed evaluation of which needs to be realized in future investigations.

Previous studies (see, e.g., Abdu 2012) have pointed out that disturbance electric fields could be present over equatorial region for space weather disturbances represented

by AE activity as low as ~ 100 nT and higher, and the probability of occurrence of such disturbances in the sunset sector over Brazil could vary on an average from 20% during solar minimum to 60% during solar maximum. For this reason, the short-term variability arising from space weather-related disturbance electric fields should be considered to be an important component of the overall variability in the ESF/EPB occurrence.

Another important component of the PRE/ESF variability may operate through the E region. In this case, the longitudinal gradient in the E layer conductivity across the sunset terminator is modified by E layer winds (as explained in Section 1.1) that may be modified by nonlinear interaction between the planetary/UFK waves and tides. The E layer conductivity longitudinal gradient so modified has been shown to be a critical parameter in controlling the amplitude and phase of the PRE vertical drift (Abdu and Brum 2009). The results presented in Section 2.2 (supported by results from previous studies) have shown that the PRE vertical drift, and hence the ESF/EPB development, can be significantly modified through such E layer processes. Another path of a potential E layer role is through the association observed between the PRE vertical drift and the wave structure represented by the F layer height oscillations (as in Fig. 6). These oscillations present a certain degree of phase coherence on a day-to-day basis, and getting amplified towards sunset as was consistently observed in different solar activity epochs (as discussed in Section 3). The possibility of interaction between upward propagating tides and gravity waves may be thought of as a possible link in the connection observed between the F layer wave structures and the PRE vertical drift, which possibly has important consequences for the ESF/EPB variability. On these bases, the variability in the evening sector E layer, arising from nonlinear interaction involving tidal wind modes on one side and the planetary/UFK waves and gravity waves on the other side, should be considered to be an important source of ESF/EPB short-term variability, and merits added attention for future research.

As regards the item (b) above concerning the ESF/EPB variability arising from the seed perturbations, important progress has been made as discussed (though in a limited way) in Section 3. There is increasing evidence on statistical as well as case study bases that the role of upward propagating gravity waves from sources in troposphere is an important factor in the ESF/EPB variability. In case studies for evaluating the gravity wave effect on EPB generation, an important consideration should be the phasing of the gravity wave oscillations relative to the peak in the PRE vertical drift that is used to determine the maximum linear growth rate in a given situation for the R-T instability to evolve. This question is a parallel one to the two-dimensional narrative in which EPB may develop from the crest region of the upwelling due to LSWS, as pointed out in Section 1.1. The phasing of the gravity wave/LSWS with respect to the peak of PRE vertical drift appears to gain importance for EPB generation especially when the PRE vertical drift is relatively small. This situation is illustrated in the results presented in Section 3 (and mentioned in item a-iii) showing an example of ESF suppression due to the positioning in anti-phase of the PRE vertical drift peak and gravity wave oscillations that occurred on 11 October (Fig. 7). Such a situation of ESF suppression was the result of a weak PRE vertical drift whose modulation by a relatively "stronger" gravity wave amplitude was possible. On this basis, we may expect the contribution from gravity wave dynamics to the overall ESF short-term variability to depend also upon the degree of the variability in the PRE vertical drift that is known to depend also upon season, longitude, and solar activity. The ITCZ/OLR parameters (that is, the Outgoing Long Wave Radiation from Inter-Tropical Convergence Zone) have been used to represent the tropospheric convective activity as a source of gravity wave seed perturbation. It has been noted that the degree of statistical correlation between the ITCZ/OLR parameters and the irregularity distribution on global or regional scale is not always uniformly conclusive for all longitudes/seasons (see, for example, Tsunoda 2010, Su et al. 2014). It appears possible that simultaneous considerations on the associated vertical drift information (wherever available) could help understand better the observed degrees of correlations in such statistical comparisons.

The nature of the ESF short-term variability due to the TEW/meridional winds (item c) appears to have been poorly investigated. Under quiet conditions, a few studies have established their role in suppressing the ESF as mentioned in Section 4. We presented what appears to be a clear case of ESF suppression by TEW during a magnetic storm event (Fig. 8). In this respect, we need to distinguish among the cases of ESF suppression occurring at different storm phases. For example, the ESF suppression at the recovery phase of a substorm occurs due to the westward disturbance electric field associated with the over-shielding effect. In this case, the PRE vertical drift will be weakened. A westward electric field due to disturbance dynamo effect occurring in the evening hours may also suppress the ESF, which is also accompanied by reduced PRE vertical drift and F layer height. In contrast to this, during the ESF/EPB suppression by a TEW/meridional wind, the PRE vertical drift may not necessarily suffer any change or sometimes may become even enhanced if the storm (AE) intensification occurs during the PRE as was found in the case presented here. Important questions remain to be answered as to what

should be the magnitude of the PRE vertical drift to produce an instability growth rate that can dominate/prevail over the retarding/suppressing effect due to a TEW/meridional wind. This question can be answered from modeling studies supported by more observations.

Conclusions

The main conclusions of this study may be highlighted as follows:

1- The PRE vertical drift, which is a basic requirement for the post-sunset ESF/EPB development, can suffer significant short-term variability due to magnetospheric forcing in the form of penetration electric fields and disturbance dynamos electric field, as well as due to atmospheric wave disturbances in the form of planetary/Kelvin waves and gravity waves, originating from lower atmosphere.
2- An under-shielding electric field of eastward polarity, associated with auroral activity or Dst development, occurring near sunset may cause an upward vertical drift that can add to the vertical drift due to the PRE thereby favoring/enhancing the ESF/EPB development. The vertical drift velocity during the PRE may increases in proportion to an increasing intensity of the penetration electric field (under-shielding electric field of eastward polarity) occurring in the evening hours. An upper limit for this proportional relationship is uncertain, however.
3- An over-shielding electric field of westward polarity, associated with the recovery phase of an AE activity, occurring just prior to the sunset, causes a decrease (or suppression) of the PRE vertical drift, which thereby contributes to stabilize the post-sunset F layer.
4- Upward propagating planetary/Kelvin waves (especially the UFK wave) may cause large degree of modulation in the PRE vertical drift (and thereby in the post-sunset F layer heights) that may contribute to intensify, or advance the onset time of, the spread F development. The underlying mechanism is believed to be nonlinear interaction of these waves with tidal mode winds, which in turn modify the longitudinal gradient in the E layer conductivity that controls the PRE development.
5- Gravity wave-induced F layer height oscillations in the form of large-scale wave structure getting amplified towards sunset appear to be a regular feature as a precursor to post-sunset ESF/EPB that may develop when the PRE vertical drift is favorable. Additionally, there appears to be present a connection between the intensity of the PRE vertical drift and the amplitude and phase of the precursor oscillations, with implications on a possible tidal-gravity wave interaction modifying the winds in evening E layer, and thereby, modifying also the PRE development.
6- The PRE vertical drift, when weakly developed, can be suppressed or even reversed to downward by upward propagating gravity waves of large enough intensity. In this way, the gravity wave activity may even lead to suppression of the post-sunset ESF/EPB development.
7- The ESF/EPB development can be suppressed by a trans-equatorial wind during magnetic storm disturbances even when the PRE vertical drift, enhanced by a prompt penetration electric field, has larger than the normal amplitude required for such development.

There are additional aspects not addressed here, including modeling results that are essential for a more detailed understanding of the short-term variability in the EPB/ESF development, which is a highly challenging task and needs to be pursued further with the support of more diverse observational results.

Abbreviations

AE: Auroral electrojet; DDEF: Disturbance dynamo electric field; EPB: Equatorial plasma bubble; ESF: Equatorial spread F; FAC: Field aligned current; IMF: Interplanetary magnetic field; ITCZ: Inter-tropical convergence zone; OLR: Outgoing long wave radiation; PPEF: Prompt penetration electric field; PRE: Prereversal enhancement in the zonal electric field; PW: Planetary waves; SYM-H: Symmetric Ring Current; TEW: Trans-equatorial wind; TIE-GCM: Thermosphere ionosphere electrodynamics - general circulation model; UFK: Ultra-fast Kelvin waves

Acknowledgements

The author acknowledges the support received from the Sao Paulo State Foundation for Promotion of Research (FAPESP) through the Process 2016/24970-7. The author acknowledges also the support received form the Ministry of Science and Technology and Conselho Nacional de Desenvolvimento Científico e Tecnológico (CNPq) through the process: CNPq 300883/2008-0. The author wishes to thank the Coordenação de Aperfeiçoamento de Pessoal de Nível Superior (Capes) for a senior visiting professorship at ITA/DCTA. The Dst/Sym-H data were downloaded from WDC/Kyoto site. The IMF data were obtained from the website http://omniweb.gsfc.nasa.gov/from/omni_min.html. Digisonde data over Sao Luis and Fortaleza were obtained from ionospheric observatory operated by INPE.

Funding

The sources of funding are: The Ministry of Science and Technology of Brazil and CNPQ Process number: 302014/2016–0, and the Foundation for Promotion of Research in the State of Sao Paulo (FAPESP) through the Process: 2016/24970–7.

Availability of data and materials

Data sharing not applicable to this article as no datasets were generated or analyzed during the current study.

Authors' contributions

The author prepared the article, read and approved the final manuscript.

Author's information

The author holds Ph.D. degree in Ionospheric Physics. Currently he is an emeritus scientist at the National Institute for Space Research (Instituto Nacional de Pesquisas Espaciais –INPE) and a visiting professor at the Aeronautic

Technology Institute (Instituto Tecnologico de Aeronautica – ITA) at Sao Jose dos Campos, Brazil. His research interest covers: Solar-Terrestrial Physics, Space Weather, Aeronomy, Ionosphere physics and vertical coupling in the atmosphere-ionosphere system.

Competing interests

The author declares that he has no competing interest.

Publisher's Note

Received: 17 October 2017 Accepted: 7 January 2019
Published online: 01 February 2019

References

Abdu MA (2012) Equatorial spread F/plasma bubble irregularities under storm time disturbance electric fields. J Atmos Terr Phys 75-76:44–56

Abdu MA, Batista IS, Bertoni F, Reinisch BW, Kherani EA, Sobral JHA (2012) Equatorial ionosphere responses to two magnetic storms of moderate intensity from conjugate point observations in Brazil. J Geophys Res 117: A05321. https://doi.org/10.1029/2011JA017174

Abdu MA, Batista IS, Reinisch BW, de Souza JR, Sobral JHA, Pedersen TR, Medeiros AF, Schuch NJ, de Paula ER, Groves KM (2009c) Conjugate point equatorial experiment (COPEX) campaign in Brazil: electrodynamics highlights on spread F development conditions and day-to-day variability. J Geophys Res 114:A04308. https://doi.org/10.1029/2008JA013749

Abdu MA, Batista IS, Sobral JHA (1981) Some characteristics of Spread F at the magnetic equatorial station Fortaleza. J Geophys Res 86(A8):6836–6842

Abdu MA, Batista IS, Takahashi H, MacDougall J, Sobral JHA, Medeiros AF, Trivedi NB (2003) Magnetospheric disturbance induced equatorial plasma bubble development and dynamics: a case study in Brazilian sector. J Geophys Res 108:A12. https://doi.org/10.1029/2002JA009721

Abdu MA, Batista PP, Batista IS, Brum CGM, Carrasco A, Reinisch BW (2006a) Planetary wave oscillations in mesospheric winds, equatorial evening prereversal electric field and spread F. Geophys Res Lett 33, n.L07107:1–4

Abdu MA, Brum CGM (2009) Electrodynamics of the vertical coupling processes in the atmosphere-ionosphere system of the low latitude region. Earth Planets Space 61:385–395

Abdu MA, Brum CGM, Batista PP, Gururbaran S, Pancheva D, Bageston J, Batista IS, Takahashi H (2015a) Fast and ultrafast Kelvin wave modulations of the equatorial evening F region vertical drift and spread F development. Earth Planets Space 67:1. https://doi.org/10.1186/s40623-014-0143-5

Abdu MA, de Souza JR, Kherani EA, Batista IS, MacDougall JW, Sobral JHA (2015b) Wave structure and polarization electric field development in the bottomside F layer leading to postsunset equatorial spread F. J Geophys Res Space Physics 120. https://doi.org/10.1002/2015JA021235

Abdu MA, Iyer KN, de Medeiros RT, Batista IS, Sobral JHA (2006b) Thermospheric meridional wind control of equatorial spread F and evening prereversal electric field. Geophys Res Lett 33, n.L07106:1–4

Abdu MA, Kherani EA, Batista IS, Batista PP, de Paula ER, Paula FD, Sobral JHA (2009a) Gravity wave initiation of equatorial spread F/plasma bubble irregularities based on observational data from the SpreadFEx campaign. Ann Geophys 27:2607–2622

Abdu MA, Kherani EA, Batista IS, Reinisch BW, Sobral JHA (2014) Equatorial spread F initiation and growth from satellite traces as revealed from conjugate point observations in Brazil. J Geophys Res Space Phys 119. https://doi.org/10.1002/2013JA019352

Abdu MA, Kherani EA, Batista IS, Sobral JHA (2009b) Equatorial evening prereversal vertical drift and spread F suppression by disturbance penetration electric fields. Geophys Res Letts Vol 36:L19103. https://doi.org/10.1029/2009GL039919

Abdu MA, Medeiros RT, Bittencourt JA, Batista IS (1983) Vertical ionization velocities and range type spread F in the evening equatorial ionosphere. J Geophys Res 88:399–402

Abdu, M. A., P. A. B. Nogueira, A. M. Santos, J. R. de Souza, I. S Batista, and J. H. A. Sobral (2008b), Impact of disturbance electric fields in the evening on prereversal vertical drift and spread F developments in the equatorial ionosphere, Ann Geophys, in press

Abdu MA et al (2008a) Abnormal evening vertical plasma drift and effects on ESF and EIA over Brazil-South Atlantic sector during the 30 October 2003 superstorm. J Geophys Res 113:A07313. https://doi.org/10.1029/2007JA012844

Abdu MA, Nogueira PAB, Santos AM, de Saouza JR, Batista IS, Sobral JHA (2018) Ann Geophys 36:1–12

Basu S, Basu S, Groves KM, Yeh H-C, Su S-Y, Rich FJ, Sultan PJ, Keskinen MJ (2001) Response of the equatorial ionosphere in the South Atlantic region to the great magnetic storm of July 15. Geophys Res Letts 28(18):3577–3580

Batista IS, Candido CMN, Souza JR, Abdu MA, de Araujo RC, Resende LCA, Santos AM (2017) F3 layer development during quiet and disturbed periods as observed at conjugate locations in Brazil: the role of the meridional wind. J Geophys Res Space Phys 122 https://doi.org/10.1002/2016JA023724

Blanc M, Richmond AD (1980) The ionospheric disturbance dynamo. J Geophys Res 85:1669–1686

Booker HG, Wells HW (1938) Scattering of radio waves in the F region of ionosphere. Terr Mag Atmos Electr 43:249

Carter BA, Yizengaw E, Pradipta R, Retterer JM, Groves K, Valladares C, Caton R, Bridgwood C, Norman R, Zhang K (2016) Global equatorial plasma bubble occurrence during the 2015 St. Patrick's Day storm. J Geophys Res Space Phys 121:894–905. https://doi.org/10.1002/2015JA022194

Dungey JW (1956) Convective diffusion in the equatorial F-region. J Atmos Terr Phys 9:304–310

Eccles JV, Maurice JPS, Schunk RW (2015) Mechanisms underlying the prereversal enhancement of the vertical plasma drift in the low-latitude ionosphere. J. Geophys. Res Space Phys 120:4950–4970. https://doi.org/10.1002/2014JA020664

Fagundes PR, Bittencourt JA, Abalde JR, Sahai Y, Bolzan MJA, Pillat VG, Lima WLC (2009) F layer postsunset height rise due to electric field prereversal enhancement: 1. Traveling planetary wave ionospheric disturbance effects. J Geophys Res 114:A12321. https://doi.org/10.1029/2009JA014390

Farley DT, Balsley BB, Woodman RF, McClure JP (1970) Equatorial spread F: implications of VHF radar observations. J Geophys Res 75:7199–7210

Farley DT, Bonelli E, Fejer BG, Larsen ME (1986) The prereversal enhancement of the zonal electric field in the equatorial ionosphere. J Geophys Res 91:13,723–13,728

Fejer BG (2011) Low latitude ionospheric electrodynamics. Space Sci Rev 158: 145–166. https://doi.org/10.1007/s11214-010-9690-7

Fejer BG, Jensen JW, Su S-Y (2008) Seasonal and longitudinal dependence of equatorial disturbance vertical plasma drifts. Geophys Res Letts 35:L20106. https://doi.org/10.1029/2008GL035584

Fejer BG, Scherliess L (1995) Time dependent response of equatorial ionospheric electric fields to magnetospheric disturbances. Geophys Res Letts 22:7,851–7,7854

Fejer BG, Scherliess L, de Paula ER (1999) Effects of the vertical plasma drift velocity on the generation and evolution of equatorial spread F. J Geophys Res 104:19854–19869

Fesen CG, Crowley G, Roble RG, Richmond AD, Fejer BG (2000) Simulation of the pre-reversal enhancement in the low latitude vertical ion drifts. Geophys Res Letts 27(13):1851–1854. https://doi.org/10.1029/2000GL000061

Forbes JM (1996) Planetary waves in the thermosphere–ionosphere system. J Geomagn Geoelectr 48:91–98

Fritts DC, Vadas SL (2008) Gravity wave penetration into the thermosphere: sensitivity to solar cycle variations and mean winds. Ann Geophys 26:3841–3861. https://doi.org/10.5194/angeo-26-3841

Haerendel G (1973) Theory of equatorial spread F, preprint Max-Planck-Instit. für extra-terr. Phys., Garching bei Munchen, Germany.

Hanson WB, Sanatani S (1971) Relationship between Fe+ ions and equatorial spread F. J Geophys Res 76:7761–7768

Heelis RA, Crowley G, Rodrigues F, Reynolds A, Wilder R, Azeem I, Maute A (2012) The role of zonal winds in the production of a pre-reversal enhancement in the vertical ion drift in the low latitude ionosphere. J Geophys Res 117: A08308. https://doi.org/10.1029/2012JA017547

Heelis RA, Kendall PC, Moffet RJ, Windle DW, Rishbeth H (1974) Electrical coupling of the E- and F-regions and its effects on the F region drifts and winds. Planet Space Sci 22:743–756. https://doi.org/10.1016/0032-0633(74)90144-5

Huang C-S, Hairston MR (2015) The post sunset vertical plasma drift and its effects on the generation of equatorial plasma bubbles observed by the C/NOFS satellite. J. Geophys. Res Space Physics 120:2263–2275. https://doi.org/10.1002/2014JA020735

Huang CS, Kelley MC, Hysell DL (1993) Nonlinear Rayleigh-Taylor instabilities, atmospheric gravity waves and equatorial spread F. J Geophys Res 98:15631. https://doi.org/10.1029/93JA00762

Hysell DL, Kudeki E (2004) Collisional shear instability in the equatorial F region ionosphere. J Geophys Res 109:A11301. https://doi.org/10.1029/2004JA010636

Kelley MC, Fejer BG, Gonzales CA (1979) An explanation for anomalous equatorial ionospheric electric fields associated with a northward turning of the interplanetary magnetic field. Geophys Res Letts 6:301–304
Kikuchi T, Hashimoto KK (2016) Transmission of the electric fields to the low latitude ionosphere in the magnetosphere-ionosphere current circuit. Geosci Letts 3:4. https://doi.org/10.1186/s40562-016-0035-6
Kikuchi T, Luhr H, Kitamura T, Saka O, Schlegel K (1996) Direct penetration of the polar electric field to the equator during DP2 event as detected by the auroral and equatorial magnetometer chains and the EISCAT radar. J Geophys Res 101:17,161–17,173
Kudeki E, Bhattacharyya S (1999) Post sunset vortex in equatorial F-region plasma drifts and implications for bottom side spread-F. J Geophys Res 104:28163–28170
Li G, Ning B, Abdu MA, Wan W, Hu L (2012) Precursor signatures and evolution of post-sunset equatorial spread-F observed over Sanya. J Geophys Res 117: A08321. https://doi.org/10.1029/2012JA017820
Li G, Otsuka Y, Ning B, Abdu MA, Yamamoto M, Wan W, Liu L, Abadi P (2016) Enhanced ionospheric plasma bubble generation in more active ITCZ. Geophys Res Letts 43. https://doi.org/10.1002/2016GL068145
Li G et al (2010) Longitudinal development of low-latitude ionospheric irregularities during the geomagnetic storms of July 2004. J Geophys Res 115:A04304. https://doi.org/10.1029/2009JA014830
Liu G, England SL, Immel TJ, Kumar KK, Ramkumar G, Goncharenko LP (2012) Signatures of the 3-day wave in the low-latitude and midlatitude ionosphere during the (January 2010) URSI World Day campaign. J Geophys Res 117: A06305. https://doi.org/10.1029/2012JA017588
Lyon AJ, Skinner NJ, Wright RW (1961) Equatorial spread F at Ibadan, Nigeria. J Atmos Terrest Phys 21:100. https://doi.org/10.1016/0021-9169(61)90104-0
Manju G, Devasia CV, Sridharan R (2007) On the seasonal variations of the threshold height for the occurrence of equatorial spread F during solar minimum and maximum years. Ann Geophys 25:855–861
Maruyama T (1988) A diagnostic model for equatorial spread F, 1. Model description and application to electric field and neutral wind effects. J Geophys Res 93(A12):14611–14622
Maruyama T, Saito S, Kawamura M, Nozaki K, Krall J, Huba JD (2009) Equinoctial asymmetry of a low-latitude ionosphere-thermosphere system and equatorial irregularities: evidence for meridional wind control. Ann Geophys 27:2027–2034
McClure JP, Singh S, Bamgboye DK, Johnson FS, Kil H (1998) Occurrence of equatorial F region irregularities: evidence for tropospheric seeding. J Geophys Res 103:29,119–29,135
Nishida A (1971) DP 2 and polar substorm. Planet Space Sci 19:205–221
Pancheva D, Haldoupis C, Meek CE, Manson AH, Mitchell NJ (2003) Evidence of a role for modulated atmospheric tides in the dependence of sporadic E layers on planetary waves. J Geophys Res 108(A5):1176
Richmond AD, Peymirat C, Roble RG (2003) Long-lasting disturbances in the equatorial ionospheric electric field simulated witha coupled magnetosphere-ionosphere-thermosphere model. J Geophys Res 108(A3): 1118. https://doi.org/10.1029/2002JA009758
Rishbeth H (1971) Polarization fields produced by winds in the equatorial F region. Planet Space Sci 19:357–369. https://doi.org/10.1016/0032-0633(71)90098-5
Rodrigues FS, Crowley G, Heelis RA, Maute A, Reynolds A (2012) On TIE-GCM simulation of the evening equatorial plasma vortex. J Geophys Res 117: A05307. https://doi.org/10.1029/2011JA017369
Rottger J (1981) Equatorial spread F by electric field and atmospheric gravity wave generated by thunderstorms. J Atmos Terr Phys 43:453. https://doi.org/10.1016/0021–9169(81)90108–2
Salby ML, Garcia RR (1987) Transient response to localized episodic heating in the tropics. Part I: excitation and short-time near-field behavior. J Atmos Sci 44:458–498
Sastri JH (1988) Equatorial electric fields of ionospheric disturbance dynamo origin. Ann Geophys 6(6):635–642
Scannapieco AJ, Ossakow SL (1976) Nonlinear equatorial spread F. Geophys Res Letts 3:451–454
Scherliess L, Fejer BG (1997) Storm time dependence of equatorial disturbance dynamo zonal electric field. J Geophys Res 102:24037
Smith JM, Rodrigues FS, Fejer BG, Milla MA (2016) Coherent and incoherent scatter radar study of the climatology and day-to-day variability of mean F region vertical drifts and equatorial spread F. J Geophys Res Space Phys 121: 1466–1482. https://doi.org/10.1002/2015JA021934
Sreeja V, Vineeth C, Pant TK, Ravindran S, Sridharan R (2009) Role of gravity wavelike seed perturbations on the triggering of ESF – a case study from unique day-glow observations. Ann Geophys 27:313–318
Su S-Y, Liu CH, Chao CK (2017) Post-midnight equatorial irregularity distributions and vertical drift velocity variations during solstices. Adv. Space Res in press 2017
Su S-Y, Wu C, Liu C (2014) Correlation between the global occurrences of ionospheric irregularities and deep atmospheric convective clouds in the Intertropical Convergence Zone (ITCZ). Earth Planets Space 66:134
Sultan PJ (1996) Linear theory and modeling of the Rayleigh-Taylor instability leading to the occurrence of equatorial spread F. J Geophys Res 101:26875–26891
Takahashi H, Wrasse CM, Fechine J, Pancheva D, Abdu MA, Batista IS, Lima LM, Batista PP, Clemesha BR, Schuch NJ, Shiokawa K, Gobbi D, Mlynczak MG, Russel JM (2007) Signature of ultra-fast Kelvin waves in the equatorial middle atmosphere and ionosphere. Geophys Res Lett 34:L11108
Takahashi H, Wrasse CM, Pancheva D, Abdu MA, Batista IS, Lima LM, Batista PP, Clemesha BR, Shiokawa K (2006) Signatures of 3–6 day planetary waves in the equatorial mesosphere and ionosphere. Ann Geophys 24:3343–3350
Thampi SV, Yamamoto M, Tsunoda RT, Otsuka Y, Tsugawa T, Uemoto J, Ishii M (2009) First observations of large-scale wave structure and equatorial spread F using CERTO radio beacon on the C/NOFS satellite. Geophys Res Letts 36: L18111. https://doi.org/10.1029/2009GL039887
Tsunoda RT (1980) Backscatter measurements of 11- cm equatorial spread-F irregularities. Geophys Res Letts 7(10):848–850
Tsunoda RT (2008) Satellite traces: an ionogram signature for large-scale wave structure and a precursor for equatorial spread F. Geophys Res Letts 35: L20110. https://doi.org/10.1029/2008GL035706
Tsunoda RT (2010) On seeding equatorial spread F during solstices. Geophys Res Letts 37:L05102. https://doi.org/10.1029/2010GL042576
Tsunoda RT (2015) Upwelling: a unit of disturbance in equatorial spread F. Prog Earth Planet Sci 2:9. https://doi.org/10.1186/s40645-015-0038-5
Tsunoda RT, Baron MJ, Owen J, Towle DM (1979) ALTAIR: an incoherent scatter radar for equatorial spread F studies. Radio Sci 14:1111–1119
Tsunoda RT, White BR (1981) On the generation and growth of equatorial backscatter plumes: 1. Wave structure in the bottomside F layer. J Geophys Res 86:3610–3616. https://doi.org/10.1029/JA086iA05p03610
Tsunoda RT, Yamamoto M, Tsugawa T, Hoang TL, Tulasi Ram S, Thampi SV, Chau HD, Nagatsuma T (2011) On seeding large-scale wave structure, equatorial spread F, and scintillations over Vietnam. Geophys Res Lett 38:L20102. https://doi.org/10.1029/2011GL049173
Tulasi Ram S, Yamamoto M, Tsunoda RT, Chau HD, Hoang TL, Damtie B, Wassaie M, Yatini CY, Manik T, Tsugawa T (2014) Characteristics of large-scale wave structure observed from African and Southeast Asian longitudinal sectors. J Geophys Res Space Phys 119:2288–2297. https://doi.org/10.1002/2013JA019712
Woodman RF (2009) Spread F – an old equatorial aeronomy problem finally resolved? Ann Geophys 27:1915–1934 www.ann-geophys.net/27/1915/2009/
Woodman RF, La Hoz C (1976) Radar observations of F region equatorial irregularities. J Geophys Res 81:5447–5466
Zalesak ST, Ossakow SL, Chadurvedi PK (1982) Nonlinear equatorial spread F: the effect of neutral winds and background Pedersen conductivity. J Geophy Res 87(A1):151–166